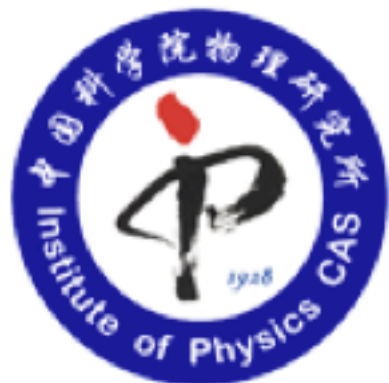


The Winter School on DFT: Theories and Practical Aspects

Institute of Physics (IOP), Chinese Academy of Sciences (CAS) in Beijing, China, Dec. 19-23, 2016.

Band Topology Theory and Topological Materials Prediction

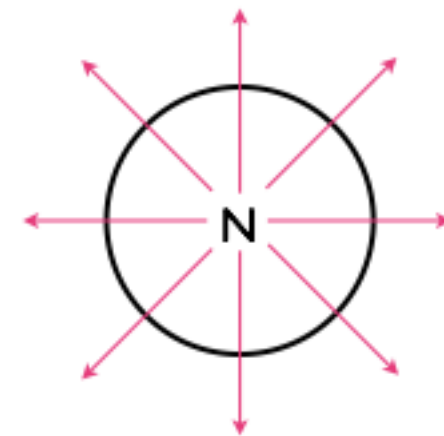


Hongming Weng (翁红明)

Institute of Physics,
Chinese Academy of Sciences



Dec. 19-23@IOP, CAS, Beijing



2016 Nobel Prize in Physics



David J. Thouless

University of Washington, Seattle, WA, USA

F. Duncan M. Haldane

Princeton University, NJ, USA

J. Michael Kosterlitz

Brown University, Providence, RI, USA

"for theoretical discoveries of topological phase transitions and topological phases of matter"

They revealed the secrets of exotic matter

TKNN number

Quantized Hall Conductance in a Two-Dimensional Periodic Potential

D. J. Thouless, M. Kohmoto,^(a) M. P. Nightingale, and M. den Nijs

Department of Physics, University of Washington, Seattle, Washington 98195

(Received 30 April 1982)

The Hall conductance of a two-dimensional electron gas has been studied in a uniform magnetic field and a periodic substrate potential U . The Kubo formula is written in a form that makes apparent the quantization when the Fermi energy lies in a gap. Explicit expressions have been obtained for the Hall conductance for both large and small $U/\hbar\omega_c$.

Because of the relation between the velocity operator and the derivatives of \hat{H} , the Kubo formula can be written as

$$\sigma_H = \frac{ie^2}{A_0 \hbar} \sum_{\epsilon_\alpha < E_F} \sum_{\epsilon_\beta > E_F} \frac{(\partial \hat{H}/\partial k_1)_{\alpha\beta} (\partial \hat{H}/\partial k_2)_{\beta\alpha} - (\partial \hat{H}/\partial k_2)_{\alpha\beta} (\partial \hat{H}/\partial k_1)_{\beta\alpha}}{(\epsilon_\alpha - \epsilon_\beta)^2}, \quad (4)$$

where A_0 is the area of the system and $\epsilon_\alpha, \epsilon_\beta$ are eigenvalues of the Hamiltonian. This can be related to the partial derivatives of the wave functions u , and gives

$$\begin{aligned} \sigma_H &= \frac{ie^2}{2\pi\hbar} \sum \int d^2k \int d^2r \left(\frac{\partial u^*}{\partial k_1} \frac{\partial u}{\partial k_2} - \frac{\partial u^*}{\partial k_2} \frac{\partial u}{\partial k_1} \right) \\ &= \frac{ie^2}{4\pi\hbar} \sum \oint dk_j \int d^2r \left(u^* \frac{\partial u}{\partial k_j} - \frac{\partial u^*}{\partial k_j} u \right), \end{aligned} \quad (5)$$

where the sum is over the occupied electron subbands and the integrations are over the unit cells in r and k space. The integral over the k -space unit cell has been converted to an integral around the unit cell by Stokes's theorem. For nonoverlapping subbands ψ is a single-valued analytic function everywhere in the unit cell, which can

only change by an r -independent phase factor θ when k_1 is changed by $2\pi/a$ or k_2 by $2\pi/b$. The integrand reduces to $\partial\theta/\partial k_j$. The integral is $2i$ times the change in phase around the unit cell and must be an integer multiple of $4\pi i$.

The problem of evaluating this quantum number remains. We have considered the potential

$$U(x, y) = U_1 \cos(2\pi x/a) + U_2 \cos(2\pi y/b), \quad (6)$$

both in the limit of a weak periodic potential ($|U| \ll \hbar\omega_c$) and in the tight-binding limit of a strong periodic potential. In the weak-potential limit the wave function can be written as a superposition of the nearly degenerate Landau functions in

Haldane Model

VOLUME 61, NUMBER 18

PHYSICAL REVIEW LETTERS

31 OCTOBER 1988

Model for a Quantum Hall Effect without Landau Levels: Condensed-Matter Realization of the “Parity Anomaly”

F. D. M. Haldane

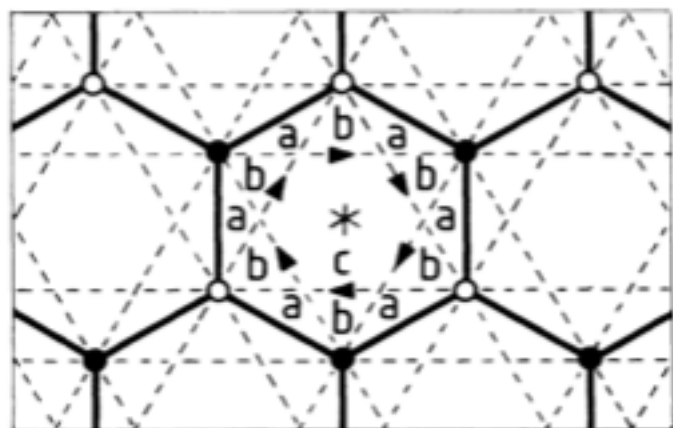
Department of Physics, University of California, San Diego, La Jolla, California 92093

(Received 16 September 1987)

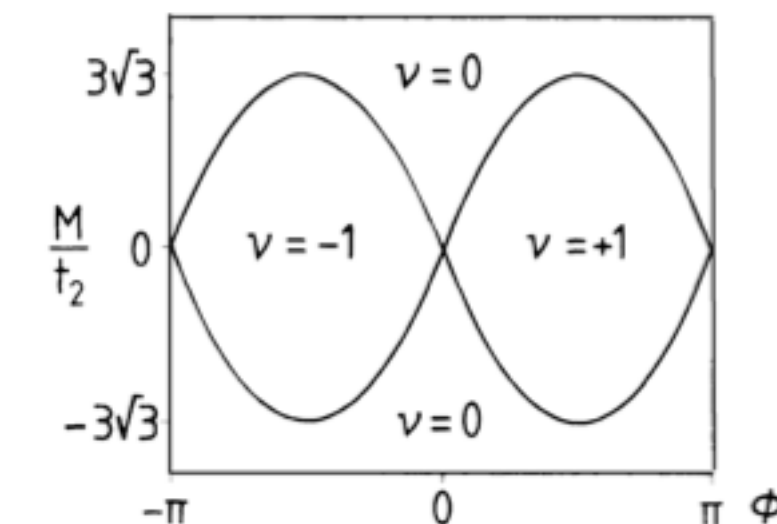
A two-dimensional condensed-matter lattice model is presented which exhibits a nonzero quantization of the Hall conductance σ^{xy} in the *absence* of an external magnetic field. Massless fermions *without spectral doubling* occur at critical values of the model parameters, and exhibit the so-called “parity anomaly” of (2+1)-dimensional field theories.

PACS numbers: 05.30.Fk, 11.30.Rd

$$H(\mathbf{k}) = 2t_2 \cos\phi \left(\sum_i \cos(\mathbf{k} \cdot \mathbf{b}_i) \right) I + t_1 \left[\sum_i [\cos(\mathbf{k} \cdot \mathbf{a}_i) \sigma^1 + \sin(\mathbf{k} \cdot \mathbf{a}_i) \sigma^2] \right] + \left[M - 2t_2 \sin\phi \left(\sum_i \sin(\mathbf{k} \cdot \mathbf{b}_i) \right) \right] \sigma^3, \quad (1)$$



a



Outline

- Band topology theory

Topological insulator (TI) and

Topological Semimetal (TS): the topological metal in 3D

TS family

- Dirac semi-metal (DSM)
- Weyl semi-metal (WSM)
- Node-line semi-metal (NLSM)
- Triply-degenerate Nodal Point semi-metal (TDNP)

Review papers on topological quantum states from first-principles calculations

Hongming Weng, Xi Dai and Zhong Fang, *MRS Bulletin* **39**, 849 (2014)

Hongming Weng, Rui Yu, Xiao Hu, Xi Dai and Zhong Fang, *Adv. Phys.* **64**, 227 (2015)

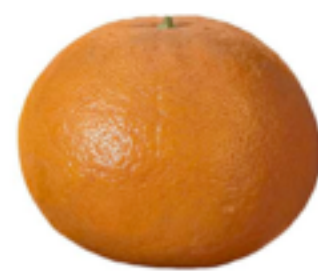
Hongming Weng, Xi Dai and Zhong Fang, *J. Phys.: Condens. Matter* **28**, 303001 (2016)

Topology in real space



I. Topological invariant

Number of holes enclosed by
compact surface: genus



$g=0$



$g=1$



$g=2$

3D number of hole



$n=0$



$n=3$

ID number of knot



$s=2$



$s=1$

2D number of surface

Continuous deformation
(adiabatic transformation)
coffee mug? or donut?



Gauss–Bonnet theorem

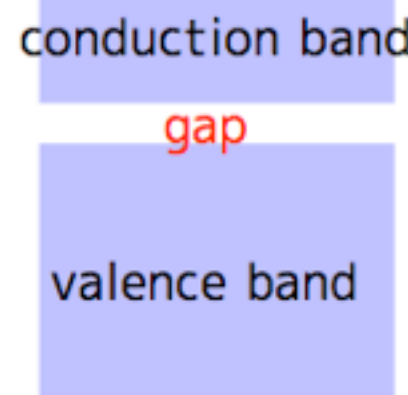
$$\frac{1}{2\pi} \int_S K dA = 2(1 - g)$$

S: compact surface
K: Gauss curvature
dA: element of area

2. Topological transition



Insulator & Metal from Band Theory

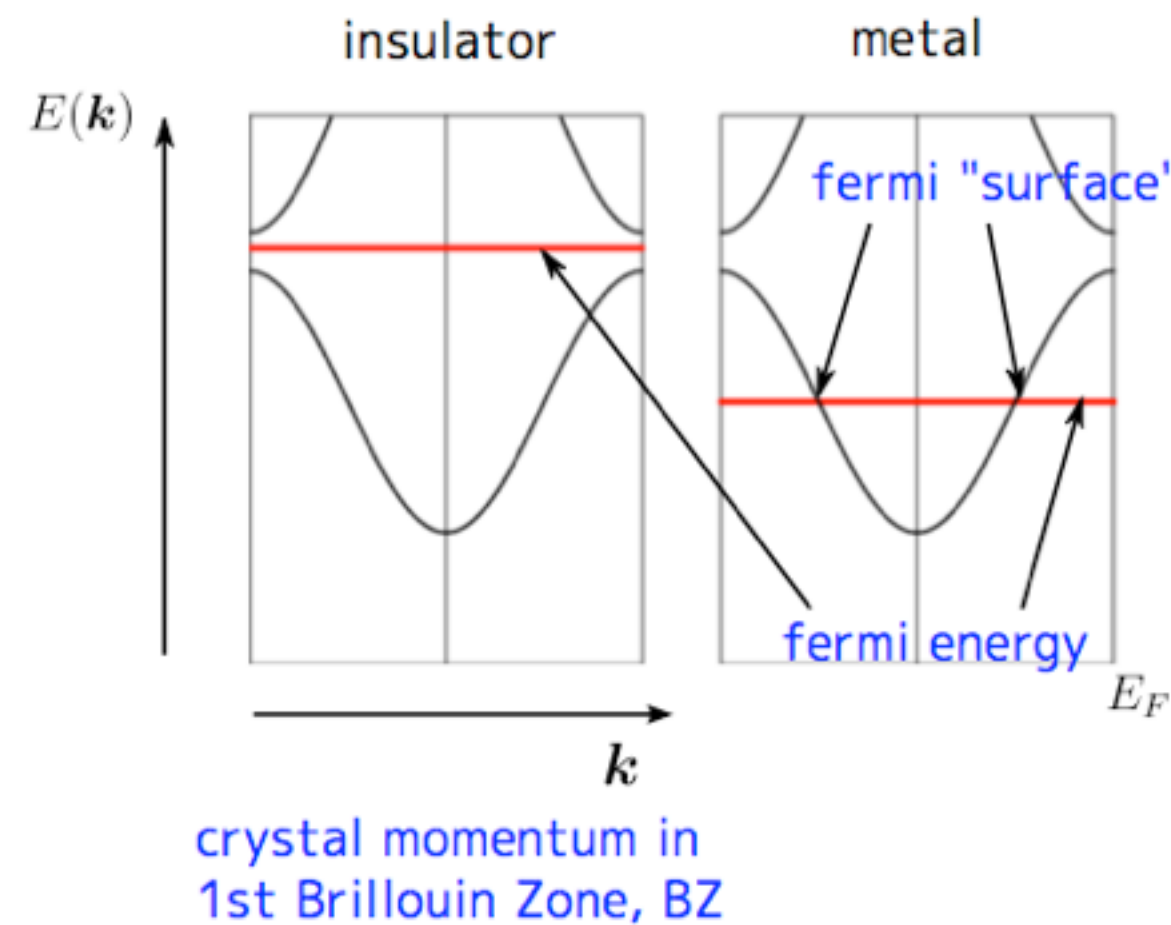


cell-periodic hamiltonian

$$\hat{H}(\vec{k}) = e^{-i\vec{k}\cdot\vec{r}} \hat{H} e^{i\vec{k}\cdot\vec{r}}$$

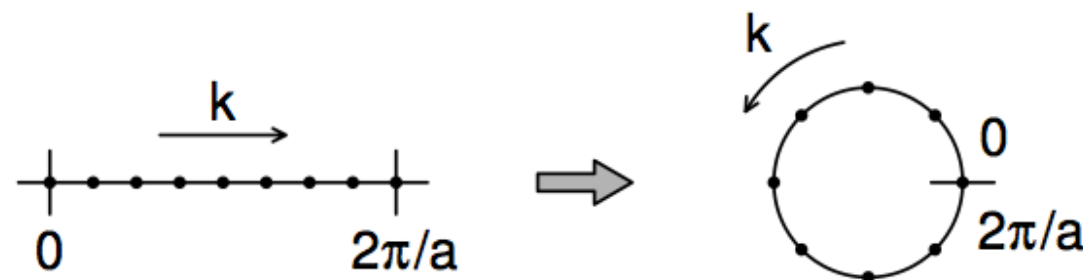
$$u_{n,\vec{k}}(\vec{r}) = e^{-i\vec{k}\cdot\vec{r}} \psi_{n,\vec{k}}(\vec{r})$$

$$\hat{H}(\vec{k})|u_{n,\vec{k}}(\vec{r})\rangle = E_n(\vec{k})|u_{n,\vec{k}}(\vec{r})\rangle$$



What are hidden/ignored?
Quantum geometrical phase
revealed by M.V. Berry.

Berry Phase and Wannier function



ID hybrid WF : $|w_0\rangle = \frac{a}{2\pi} \int dk e^{ikx} |u_k\rangle$

$$x_0 = \langle w_0 | x | w_0 \rangle$$

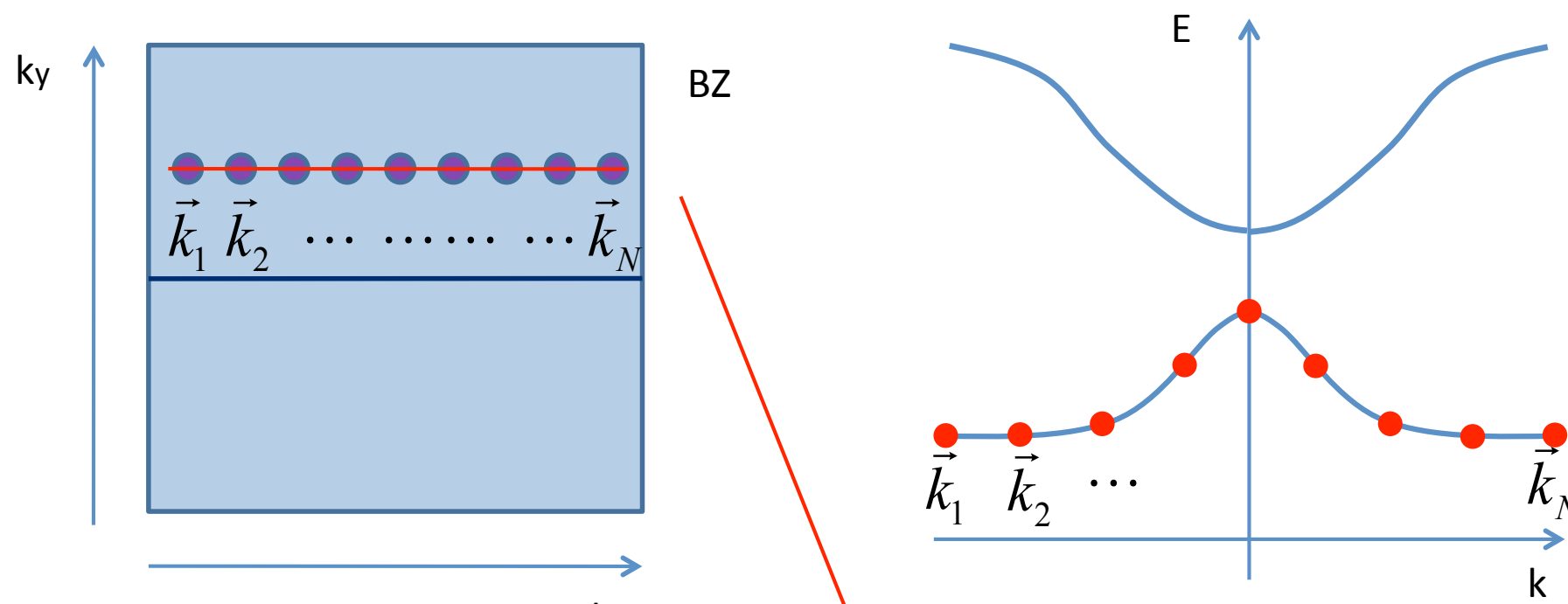
$$x|w_0\rangle = \frac{a}{2\pi} \int dk (-i\partial_k e^{ikx}) |u_k\rangle = \frac{a}{2\pi} \int dk e^{ikx} i |\partial_k u_k\rangle$$

$$x_0 = -\frac{a}{2\pi} \text{Im} \int_0^{2\pi/a} dk \langle u_k | \partial_k | u_k \rangle$$

$$x_0 = \frac{a\phi}{2\pi}$$

that is, the Berry phase ϕ introduced earlier is nothing other than a measure of the location of the Wannier center in the unit cell. The fact that ϕ was

Introduction to Berry Phase



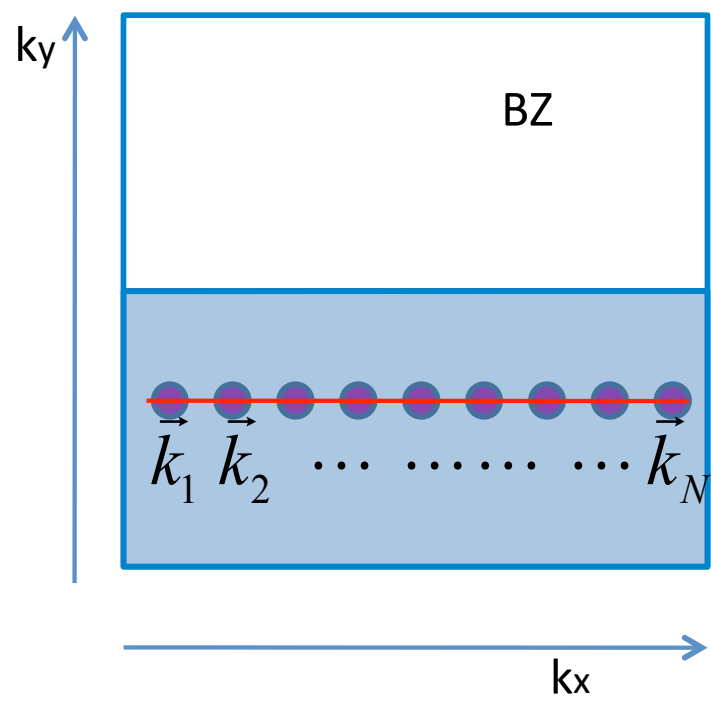
$$\langle u_{\vec{k}_1} | u_{\vec{k}_2} \rangle \langle u_{\vec{k}_2} | u_{\vec{k}_3} \rangle \cdots \cdots \langle u_{\vec{k}_{N-1}} | u_{\vec{k}_N} \rangle \langle u_{\vec{k}_N} | u_{\vec{k}_1} \rangle = A e^{i\theta(k_y)}$$

Berry connection

Meaning of the phase:
the center of the Wannier
function for 1D band insulator
or the charge center

Introduction to Berry Phase

Generalized Berry connection



Wilson loop method

Non Abelian Berry connection:

$$U_{i,i+1}^{nm}(k_y) = \langle u_{n,k_i} | u_{m,k_{i+1}} \rangle$$

$m,n=1,2$

Define the D matrix as:

$$D(k_y) = U_{1,2} U_{2,3} U_{3,4} \cdots U_{N-1,N} U_{N,1}$$

D: 2×2

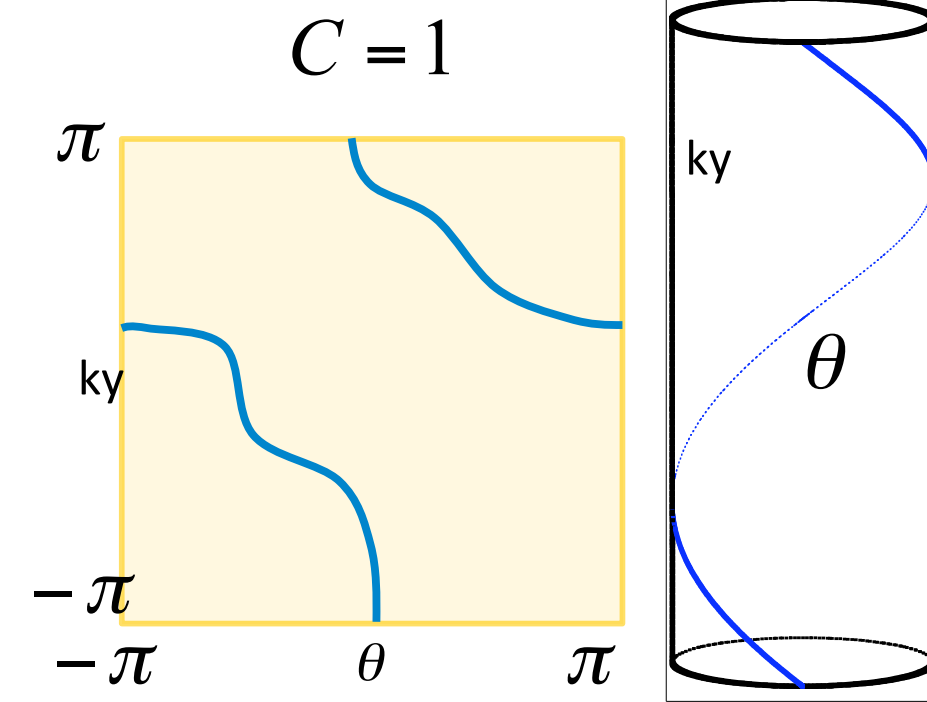
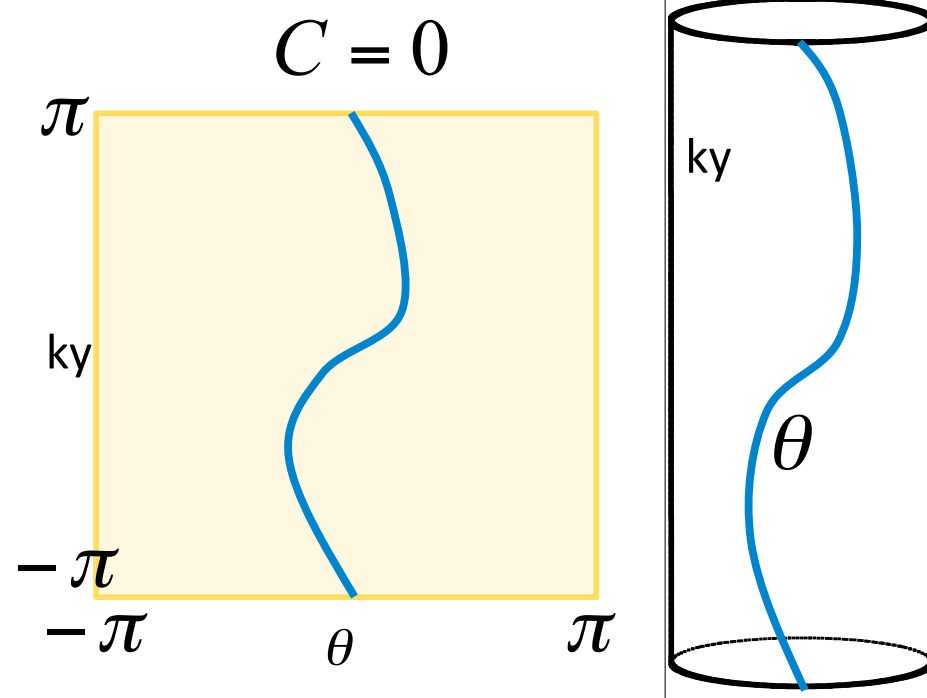
The eigenvalues of D(k_y) is $e^{i\theta_n(k_y)}$

$n=1,2$

A. Soluyanov, D. Vanderbilt, Phys. Rev. B **83**, 235401 (2011)
Yu, R., Qi, X. L., Bernevig, B., Fang, Z. & Dai, X. Phys. Rev. B **84**, 075119 (2011).

Berry Phase & Band Topology

$\theta_n(k_y)$ is the center position of the n'th Wannier function.

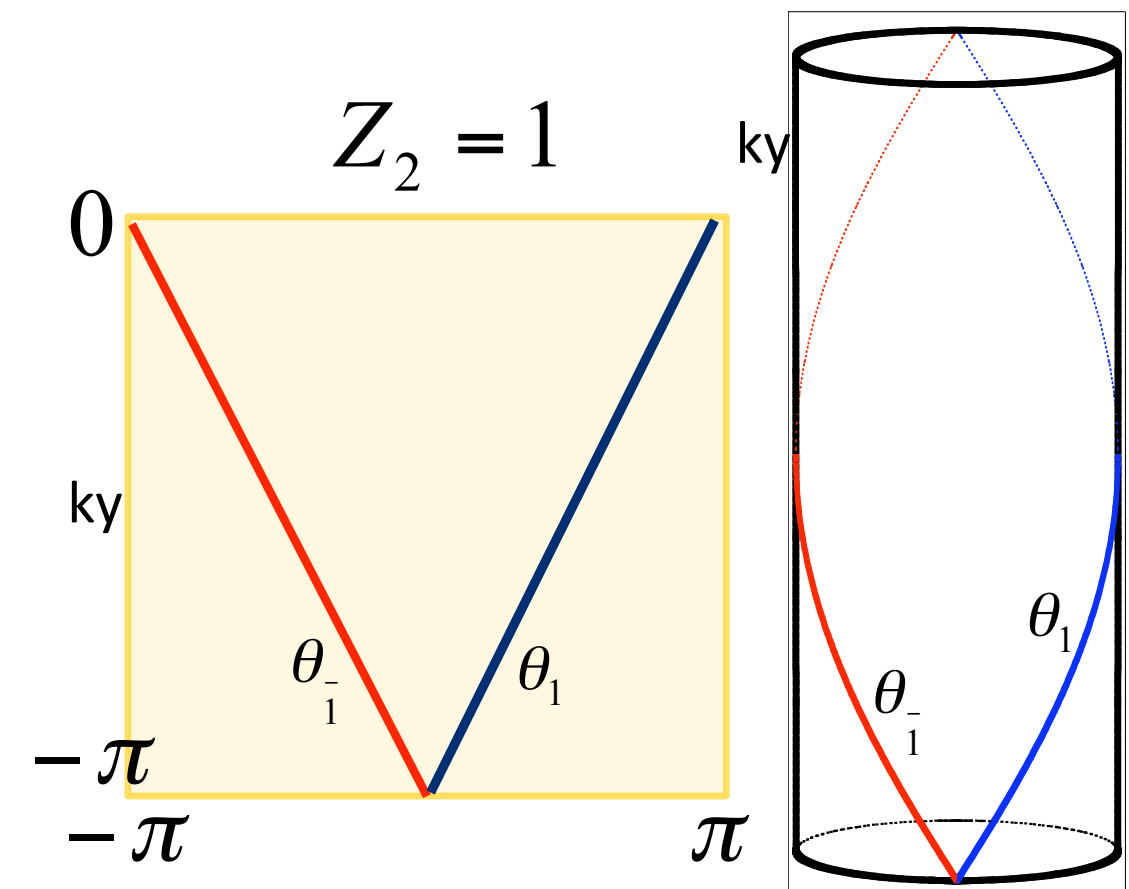
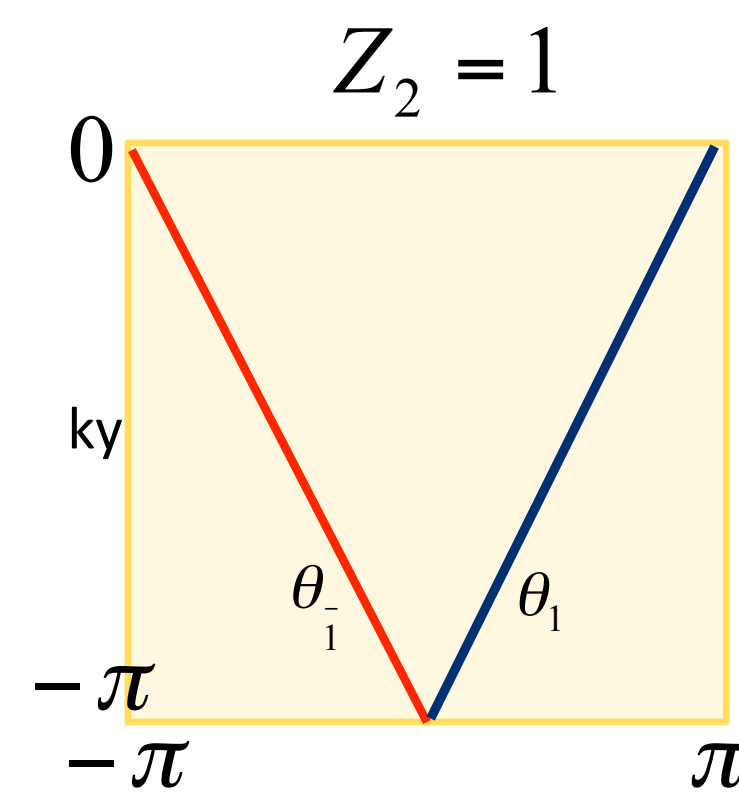
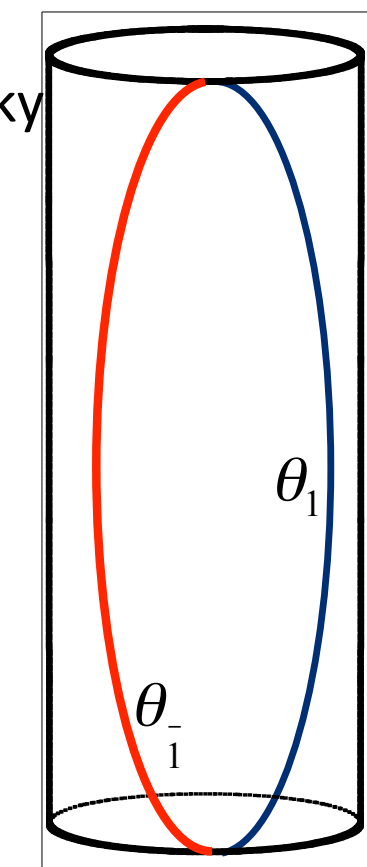
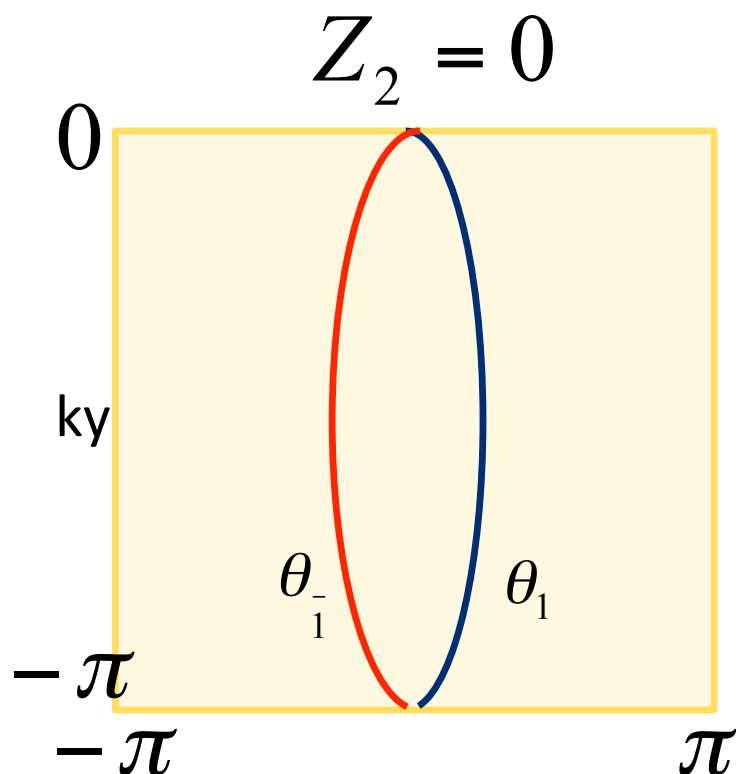


A. Soluyanov, D. Vanderbilt, Phys. Rev. B **83**,
235401 (2011)
Yu, R., Qi, X. L., Bernevig, B., Fang, Z. & Dai, X.
Phys. Rev. B **84**, 075119 (2011).

Hongming Weng, R. Yu, X. Hu, X. Dai, Z. Fang,
Adv. Phys. **64**, 227 (2015)

Berry Phase & Band Topology

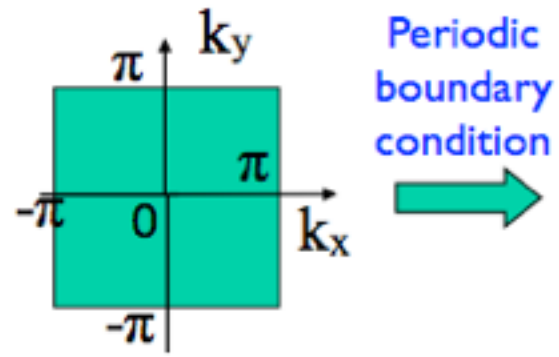
time-reversal symmetry makes $\theta(k_y)$ is doubly degenerate at $k_y=0$ and $k_y=\pi$



A. Soluyanov, D. Vanderbilt, Phys. Rev. B **83**,
235401 (2011)
Yu, R., Qi, X. L., Bernevig, B., Fang, Z. & Dai, X.
Phys. Rev. B **84**, 075119 (2011).

Hongming Weng, R. Yu, X. Hu, X. Dai, Z. Fang,
Adv. Phys. **64**, 227 (2015)

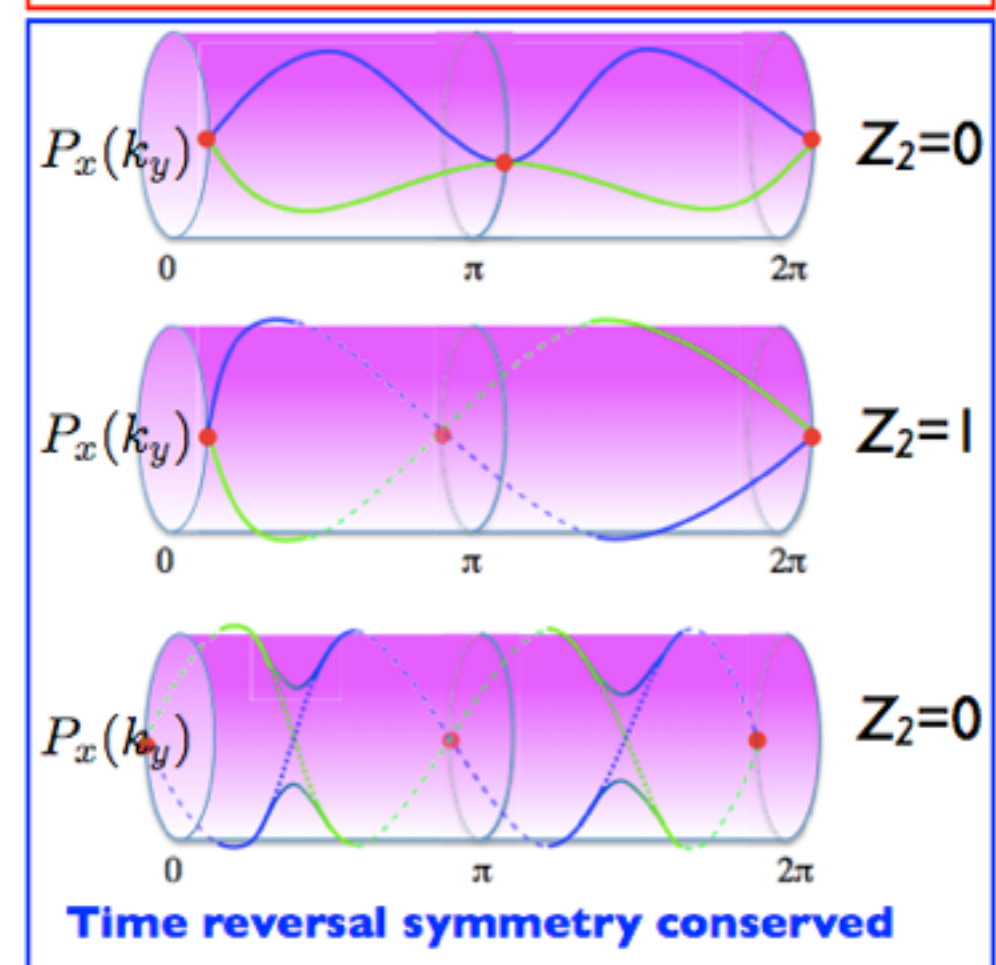
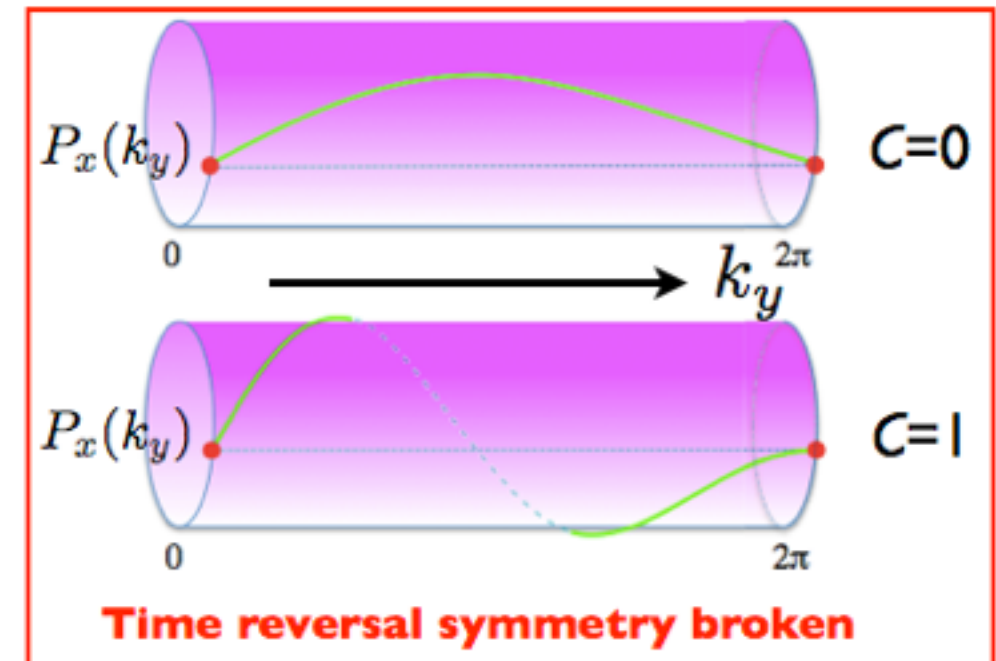
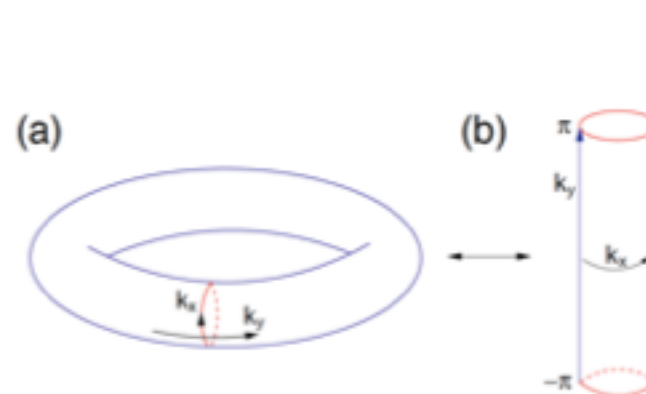
Wilson loop method for determining Topology of bands



$$\begin{aligned}
 C &= -\frac{1}{2\pi} \int \int dk_x dk_y (\partial_x A_y(k_x, k_y) - \partial_y A_x(k_x, k_y)) \\
 &= -\frac{1}{2\pi} \int_{-\pi}^{\pi} dk_y (A_y(2\pi, k_y) - A_y(0, k_y)) \\
 &\quad + \frac{1}{2\pi} \int_{-\pi}^{\pi} dk_y \partial_y \left(\int_{-\pi}^{\pi} dk_x A_x(k_x, k_y) \right) \\
 &= \frac{1}{2\pi} \int_{-\pi}^{\pi} dk_y \partial_y \left(\int_{-\pi}^{\pi} dk_x A_x(k_x, k_y) \right) \\
 &= \int_{-\pi}^{\pi} dP_x(k_y)
 \end{aligned}$$

1D hybrid Wannier Center: *x-direction only*

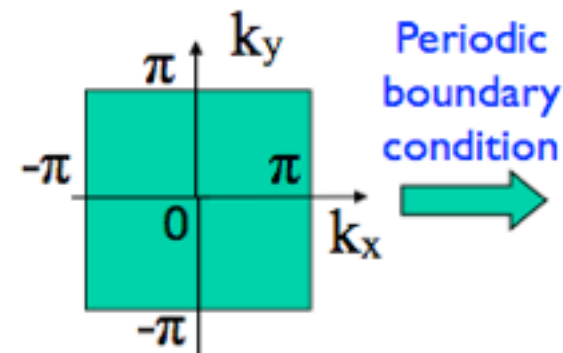
$$P_x(k_y) = \frac{1}{2\pi} \int_{-\pi}^{\pi} A_x(k_x, k_y) dk_x = \gamma(k_y)/2\pi$$



Magnetic Monopole & Band topology

$$\psi_{n\mathbf{k}}(\mathbf{r}) = e^{i\mathbf{k}\cdot\mathbf{r}} u_{n\mathbf{k}}(\mathbf{r}) e^{i\phi_n(\mathbf{k})}$$

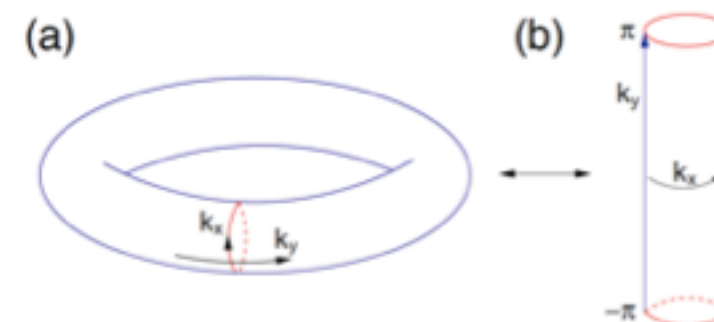
2D BZ



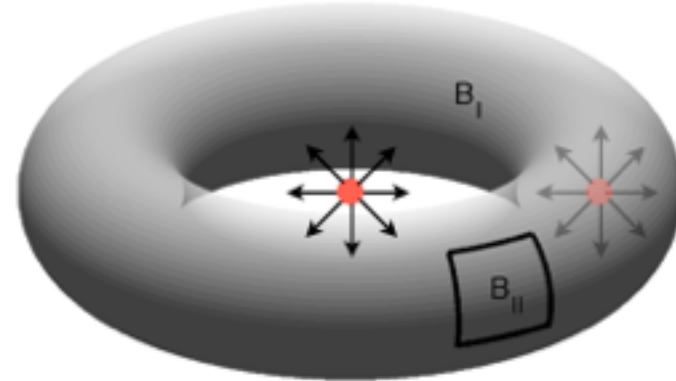
$$\begin{aligned} \phi_n &= \oint_C \vec{A}(\vec{k}) d\vec{k} \\ &= \iint_{S(c)} \Omega_z(\vec{k}) dk^2 \end{aligned}$$

$$\vec{A}(\vec{k}) = \sum_n \langle n\vec{k} | \vec{\nabla}_k | n\vec{k} \rangle$$

$$\vec{\Omega}(\vec{k}) = \vec{\nabla}_k \times \vec{A}(\vec{k})$$

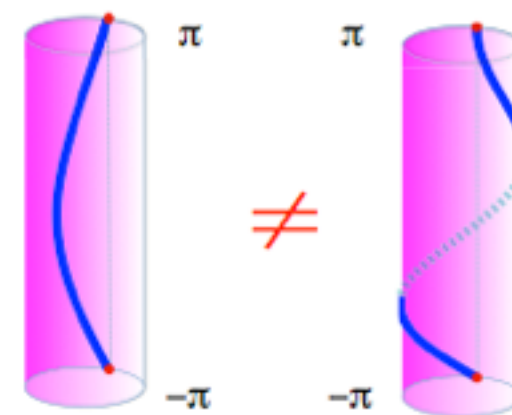


Gauss' theorem



number of monopole enclosed
by momentum space

$\phi_n(\mathbf{k})$ winding number



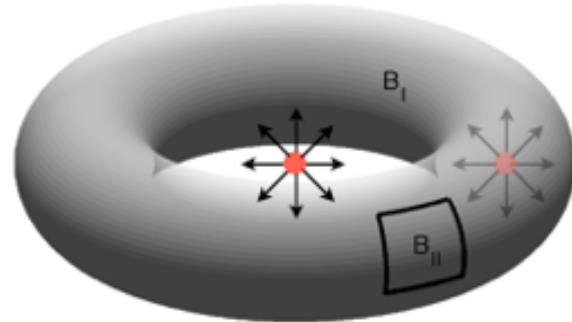
winding number



Magnetic Monopole & Band topology

Insulator vs. Metal

Gauss' theorem

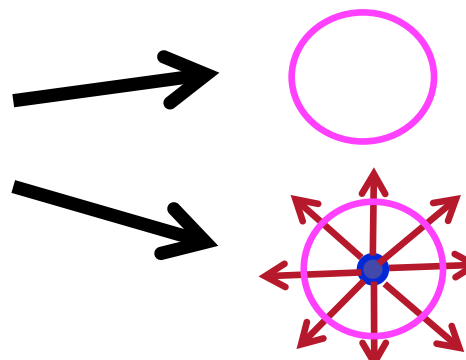


number of monopole enclosed
by momentum space

The adiabatic loop does not necessarily pass through the magnetic monopole.

$$\frac{1}{2\pi} \oint_{FS} \vec{\Omega}(k) \cdot d\vec{S}(k) = C_{FS}$$

Defined on 2D Fermi surface
of a 3D metallic system



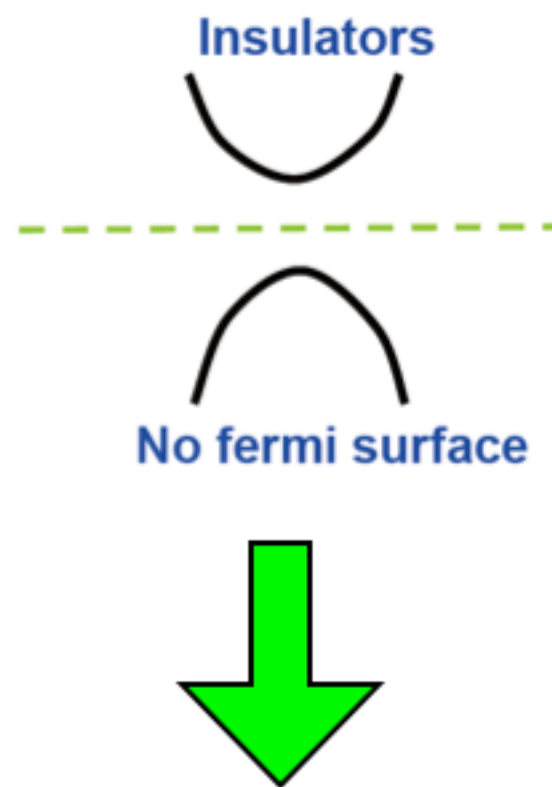
Normal metal

Topological metal

Generalized from whole Brillouin zone in *insulators* to
any closed manifold in crystal momentum space.

State of matter from Band Topology

Insulator:
no fermi surface



Normal Insulator
+
Topologically nontrivial Insulator



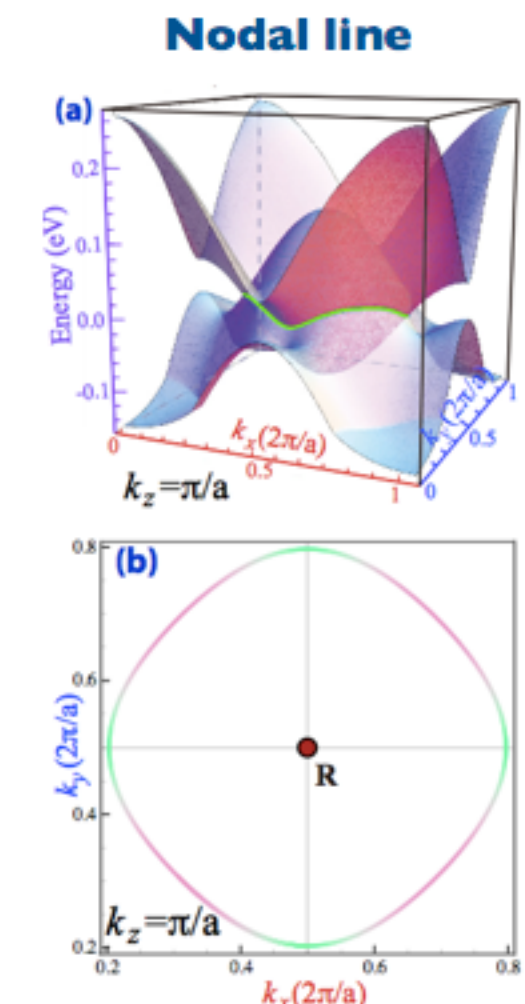
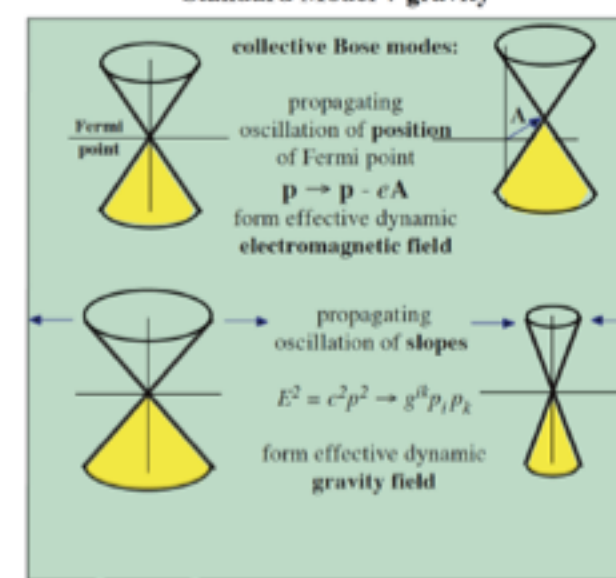
Normal Metal + Topological Semi-metal

?Metal?

Three types of Fermi surface

Semi-metal
(Dirac, Weyl)

~~Ef~~
Fermi points (in bulk)
Fermi arcs (on surface)
Standard Model + gravity



Weyl Semimetal
Dirac Semimetal
Node-line Semimetal

Extended the concept of topology to metal.

Recent Research Interests

I. Explore new Topological Quantum States

Dirac Semimetal: Na₃Bi (PRB'12, Science'14) Cd₃As₂ (PRB'13, Nat.Mater.'14)

Weyl Semimetal: HgCr₂Se₄ (PRL'11), TaAs (3xPRX'15, Nat. Phys.'15, PRL'15, Nat. Commun.'16)

Node-line Semimetal: 3D carbon crystal (PRB'15, PRL'16), Cu₃PdN(PRL'15)

Triply-Degenerated-Nodal-Point semimetal: TaN (PRB'16), ZrTe (PRB'16)

2. Understand new Topological Quantum Phenomena

**Correlated
Topological
Insulator** SmB₆ (PRL'12, Nat. Commun.'14)
 YbB₆ & YbB₁₂ (PRL'14)

3. Predict new Topological Materials

Ag₂Te (PRL'11)

ZrTe₅&HfTe₅ (PRX'14,PRX'16), MXene (PRB'15), ZrSiO (PRB'15) Large band-gap 2D TI

TIN(PRB'14)

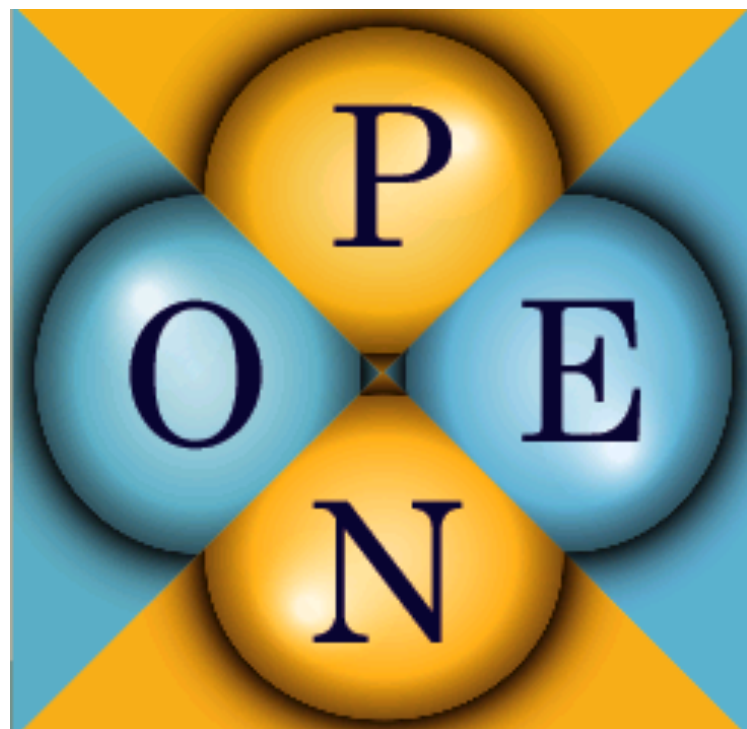
Works employed OpenMX.

Highly Efficient computational tools
is the basis

- 1, Local orbital base and pseudo-potential methods
- 2, Wannier function analysis
- 3, LDA++ methods: +Gutzwiller, +DMFT etc.
- 4, Material database

Methodology

I, Local orbital base and pseudo-potential methods



Advantage:

- + Quickly obtain electronic structure
- + from $O(N^3)$ to $O(N)$
- + spin-orbit coupling
- + structural optimization & molecular dynamic
- + non-collinear magnetism
- + structural code & easy to be extended

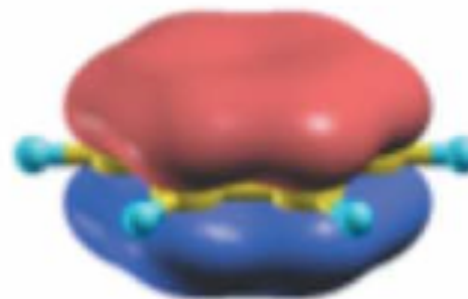
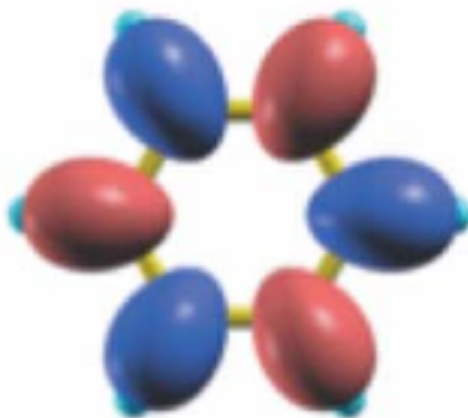
Disadvantage:

- + cut-off appro. & basis completeness
- + pseudo-potential

<http://www.openmx-square.org>

Methodology

2, Wannier function analysis



Advantage:

- + Intuitive picture;
- + accurate minimal basis;
- + highly efficient integration

Features of our code:

- + flexible projector;
- + symmetrized.

Hongming Weng,* T. Ozaki, and K. Terakura, Phys. Rev. B **79**, 235118 (2009)

Recent developments:

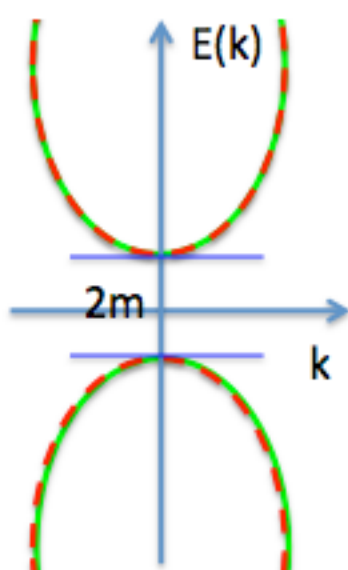
1. Boundary state calculation: slab model & Green's function method
2. Spin texture
3. Wilson loop calculation
4. Parity calculation
5. Anomalous Hall Conductivity calcualtion

Dirac & Weyl Fermion

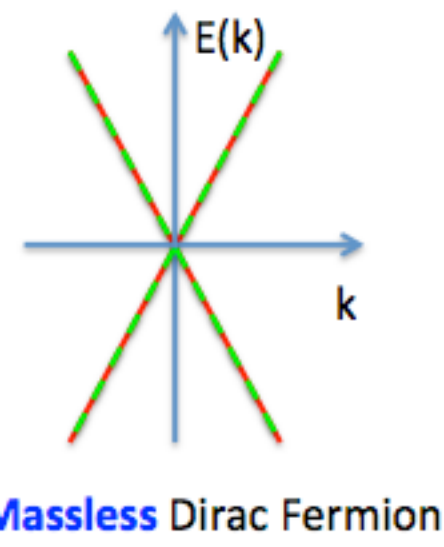
Dirac Fermion (1928) 4x4

$$\begin{pmatrix} \hat{E} - c\boldsymbol{\sigma} \cdot \hat{\mathbf{p}} & 0 \\ 0 & \hat{E} + c\boldsymbol{\sigma} \cdot \hat{\mathbf{p}} \end{pmatrix} \psi = mc^2 \begin{pmatrix} 0 & I_2 \\ I_2 & 0 \end{pmatrix} \psi$$

$$E(k) = \pm \sqrt{k^2 + m^2}$$



Massive Dirac Fermion



Massless Dirac Fermion

Massless Dirac Fermion (1929)

Weyl fermion 2x2

$$H(\vec{k}) = \vec{k} \cdot \vec{\sigma} = \begin{bmatrix} k_z & k_x - ik_y \\ k_x + ik_y & -k_z \end{bmatrix}$$

Massless Dirac Fermion: two Weyl Fermions with opposite topological charges “kiss”.

L. Balents, Weyl electrons kiss. Physics **4**, 36 (2011).

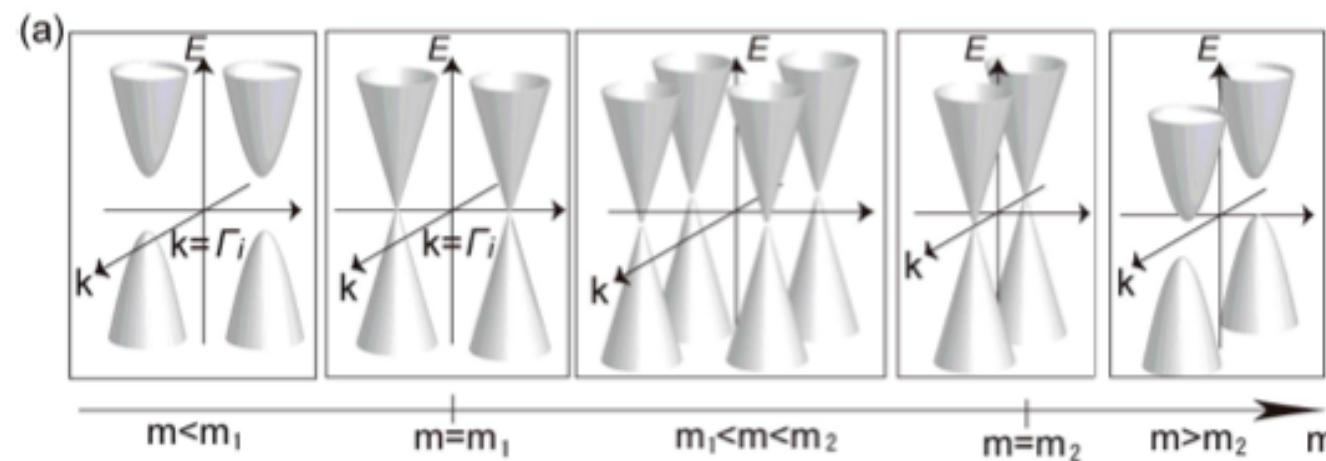
X. Wan *et al.* Phys.Rev.B **83**, 205101 (2011).

Dirac & Weyl Semimetal

Transition state between TI and NI in 3D

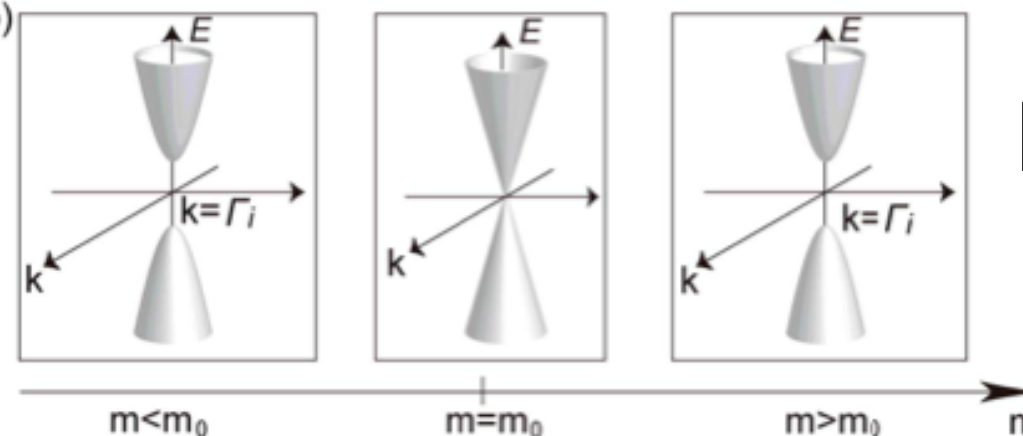
S. Murakami et al. arXiv:1006.1188
Physica E 43, 748–754 (2011)

no Inversion symmetry



Weyl nodes

with Inversion symmetry



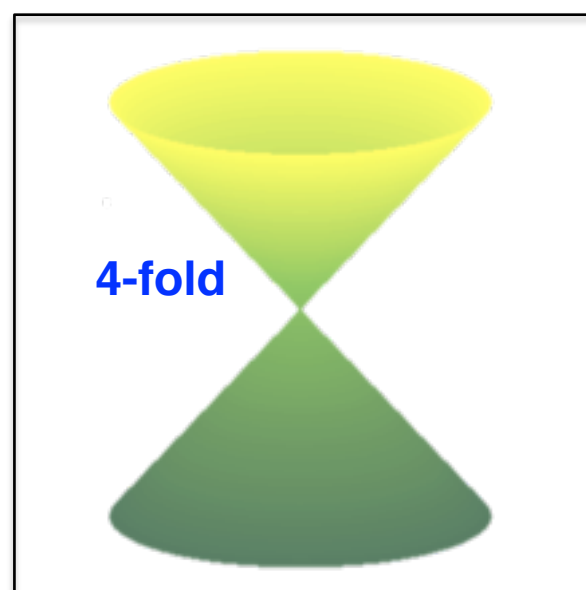
Dirac nodes

Fragile and hard to control.

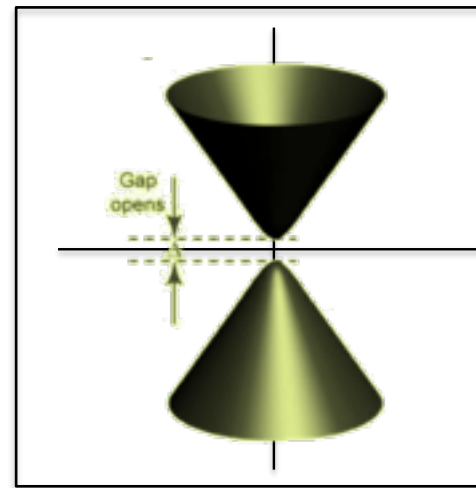
3D metal with low energy excitation behaving the same as massless Dirac/Weyl fermion.

Dirac Semimetal with Band Inversion

as “singularity point” of various topological states

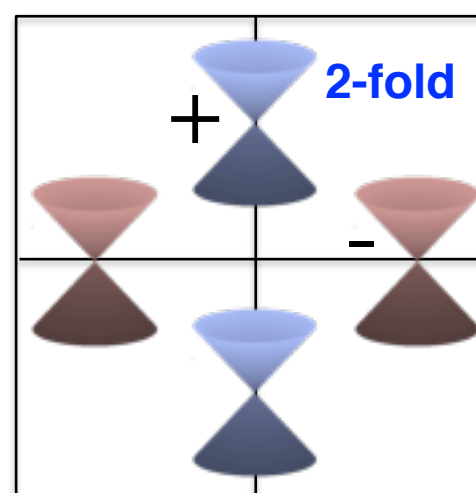


breaking
Inversion
symmetry



Noncentrosymmetric
& nonmagnetic Weyl
Semimetal

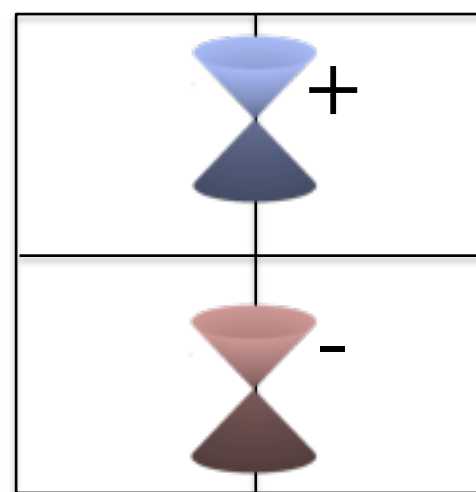
TaAs-family(PRX’15)



Na₃Bi & Cd₃As₂

The only two DSMs
widely studied
experimentally.

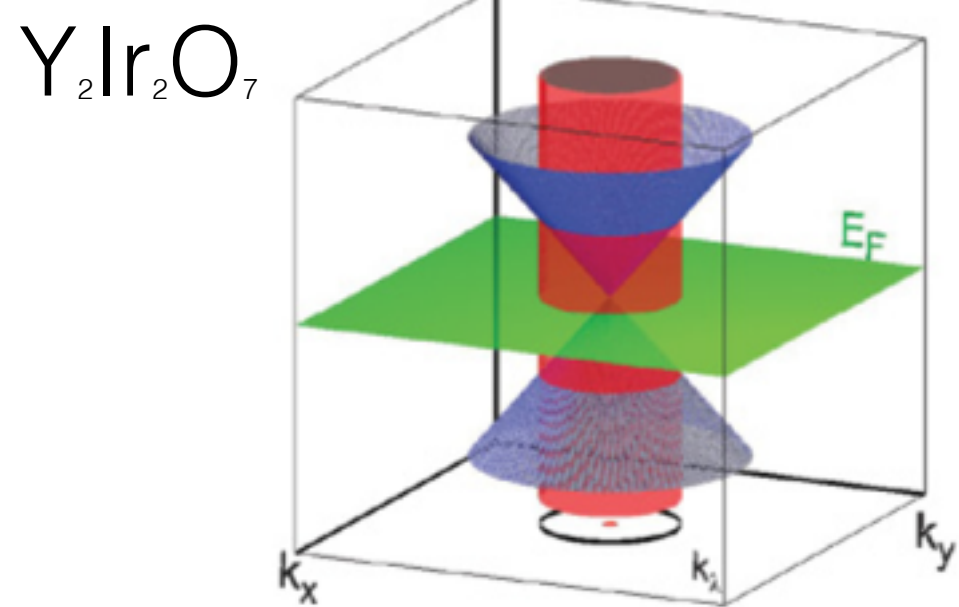
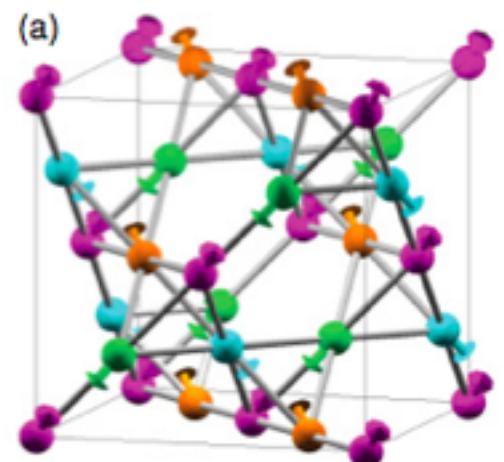
breaking
Time reversal
symmetry



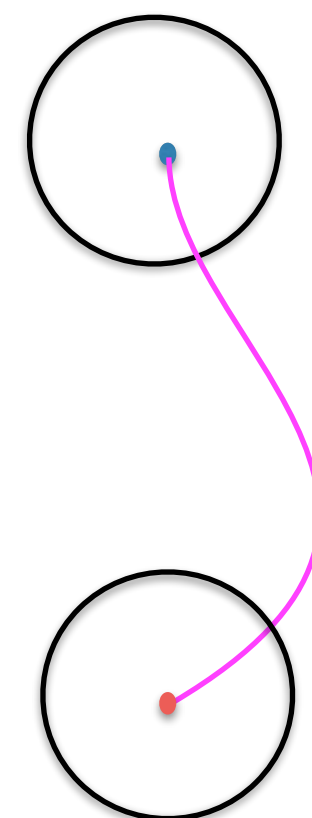
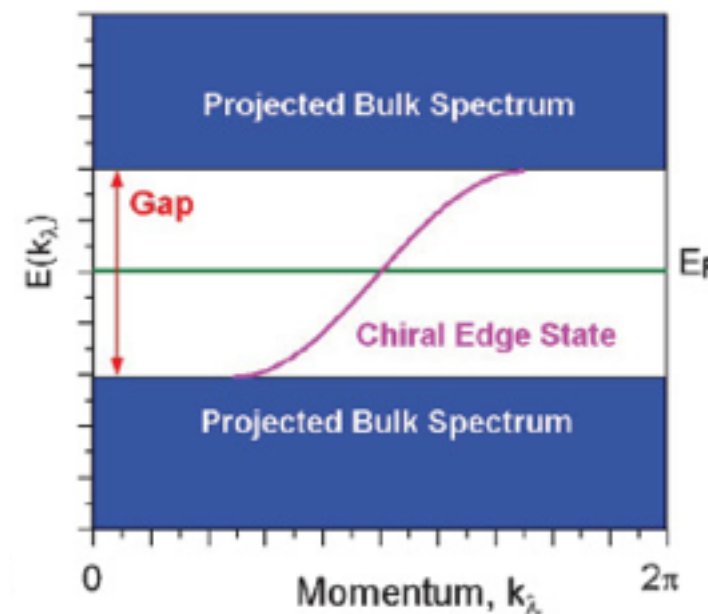
Magnetic Weyl
Semimetal

A₂Ir₂O₇ (X. Wan et al PRB’11),
HgCr₂Se₄ (PRL’11)

Fermi arcs of WSM



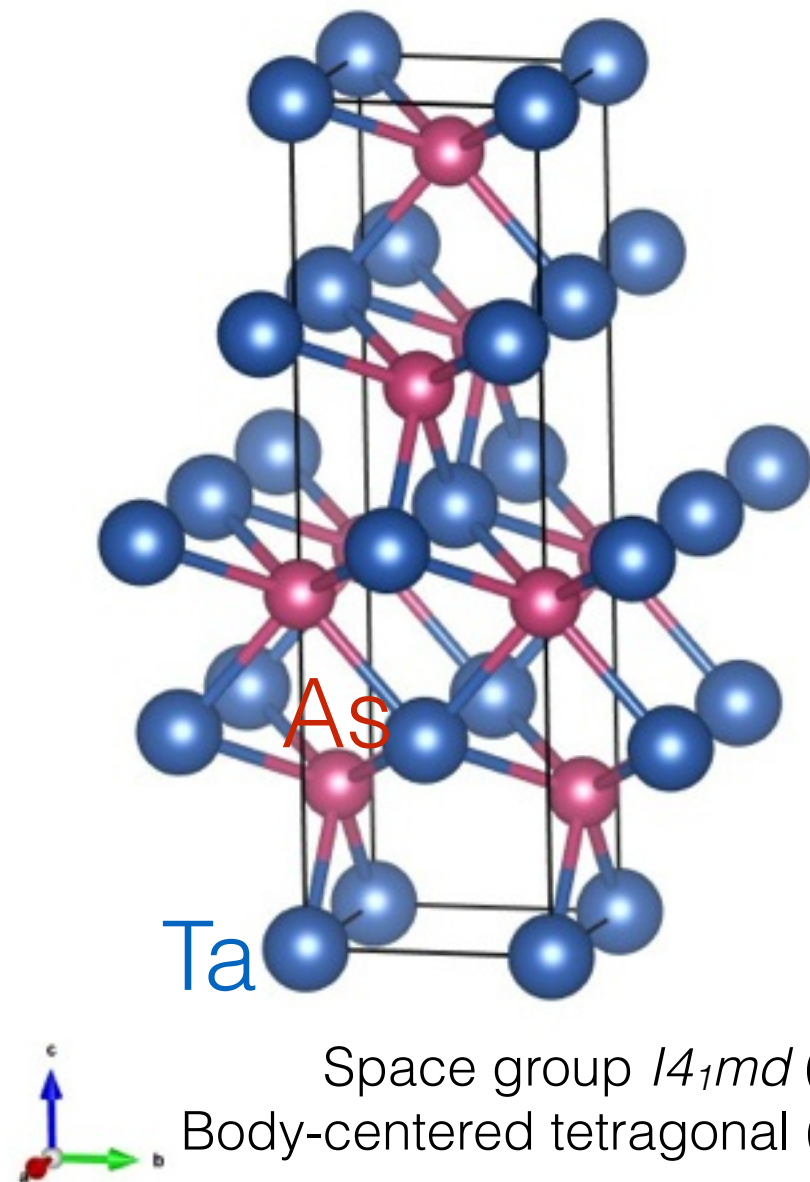
Fermi arcs on the surface



Topview

Xiangang Wan et al. Phys.Rev.B 83,205101 (2011)

Crystal structure of TaAs family



Both **Ta** and **As** are at $4a$ Wyckoff position.
 $(0,0,u)$ and $u_{\text{Ta}}=0.0$.

	a=b	c	u
TaAs	3.4348	11.641	0.417
TaP	3.3184	11.363	0.416
NbAs	3.4517	11.680	0.416
NbP	3.33242	11.37059	0.417

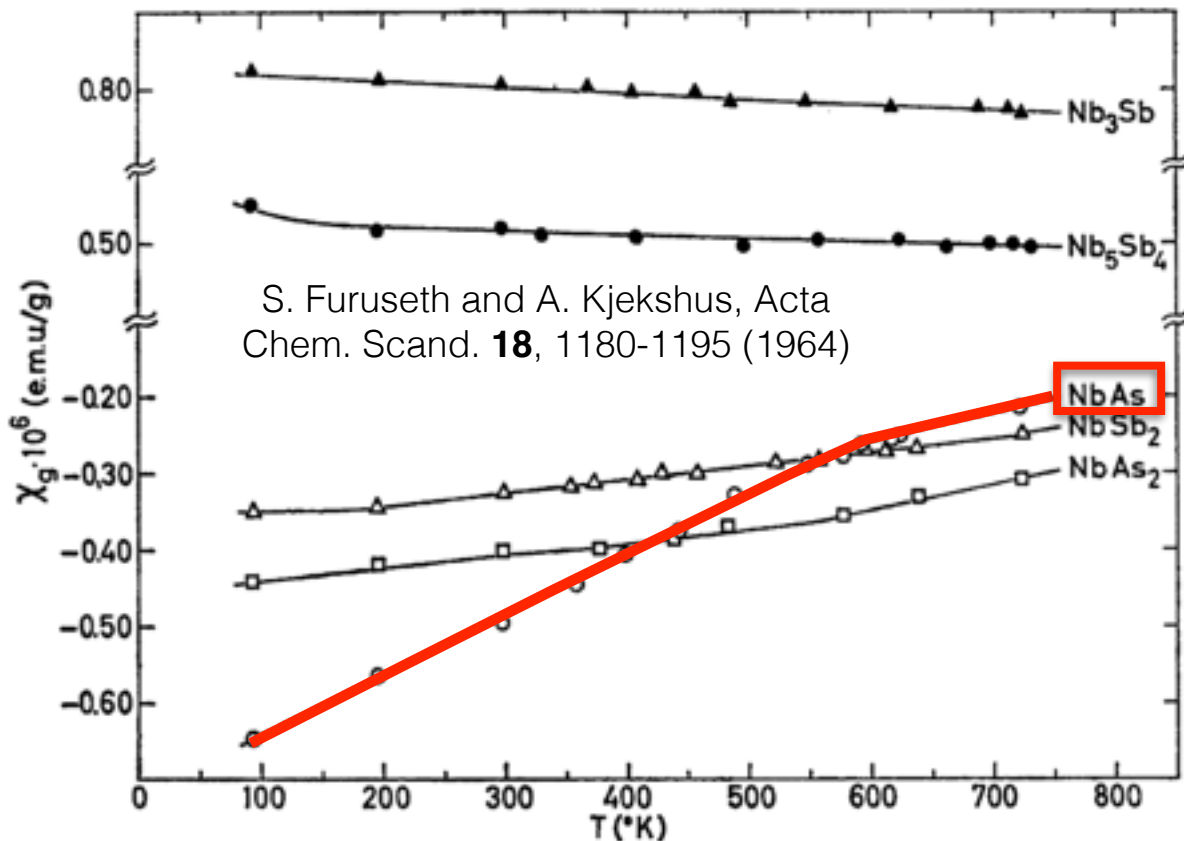
S. Furuseth, K. Seltz and A. Kjekshus,
Acta Chem. Scand. **19**, 95 (1965)

Hongming Weng*, Chen Fang, Zhong Fang, A. Bernevig, Xi Dai,
<http://arxiv.org/abs/1501.00060> posted on Dec. 31, 2014 and
Published as Phys. Rev. X 5, 011029 (2015) in March, 2015.

a similar work from Princeton group
<http://arxiv.org/abs/1501.00755> posted on Jan. 5, 2015 and
published as Nat. Commun. 6, 7373 (2015) in Jun. 2015

Known properties of TaAs family

NbAs



TaAs

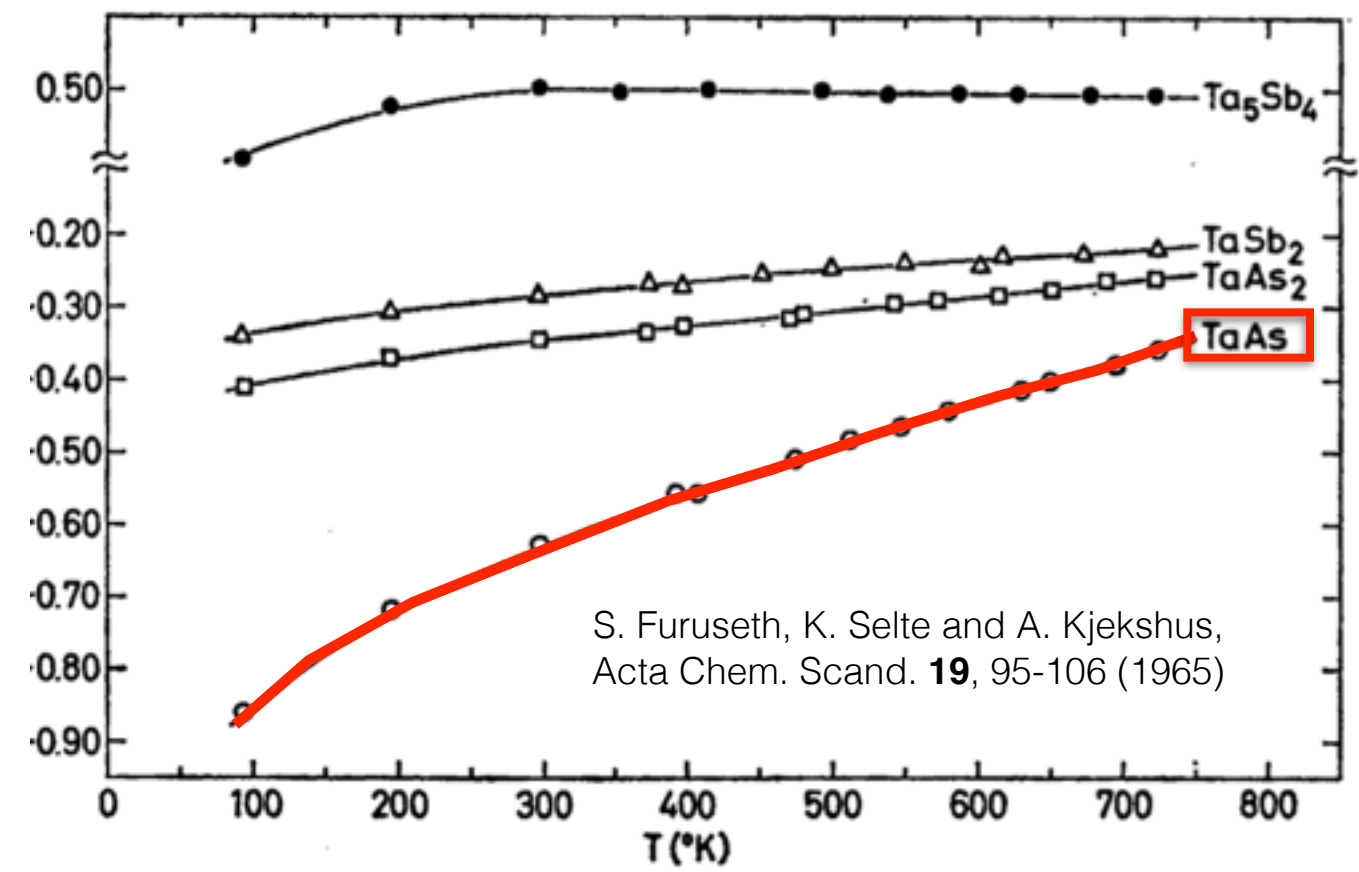


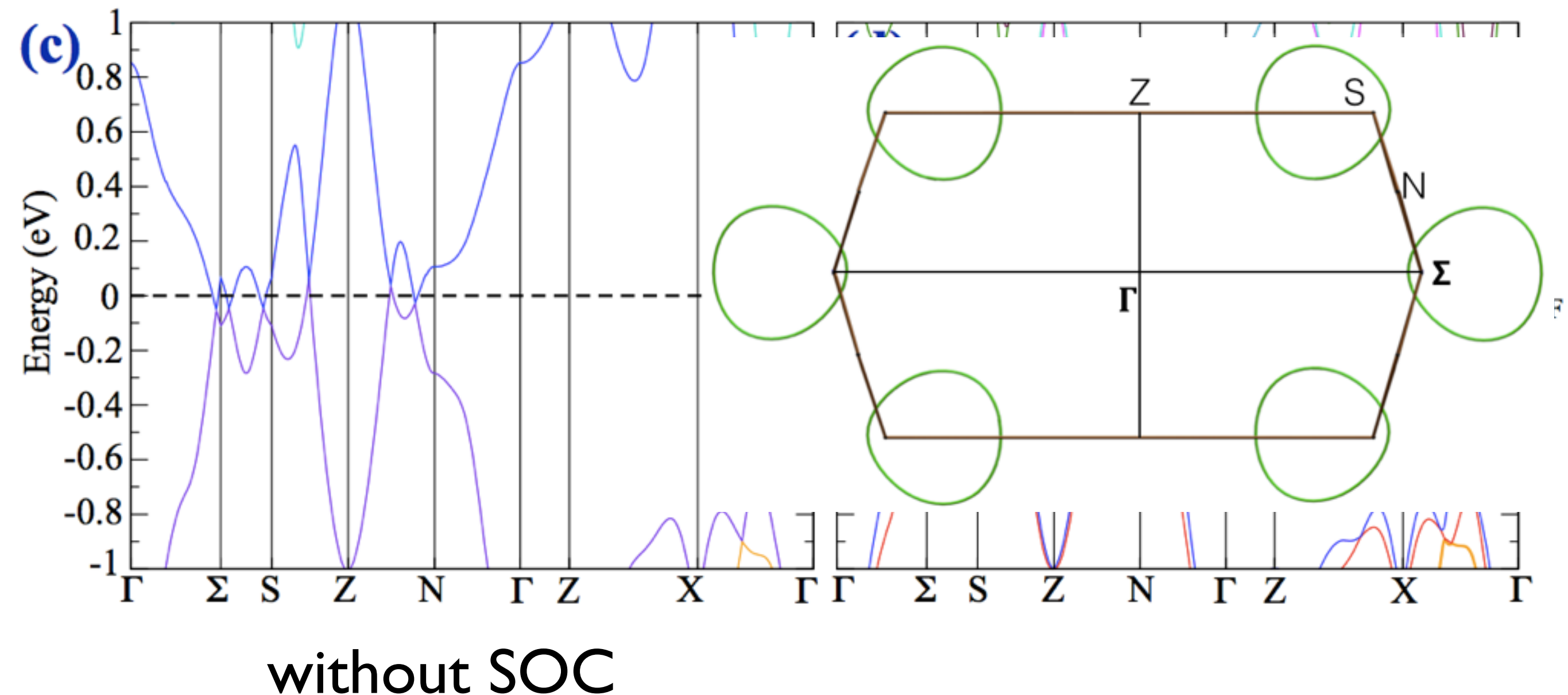
Fig. 5. The magnetic susceptibilities of NbAs , NbAs_2 , Nb_3Sb , Nb_5Sb_4 , and NbSb_2 , as a function of temperature.

TABLE V. Magnetic susceptibilities of NbP and TaP .

Compound	T (°K)	$X_g (10^{-6} \text{ cgs/g})$
NbP	78	-0.45 ± 0.03
	201	-0.57 ± 0.03
	297	-0.52 ± 0.02
	373	-0.55 ± 0.03
TaP	78	-0.70 ± 0.03
	201	-0.65 ± 0.03
	297	-0.62 ± 0.02
	373	-0.59 ± 0.02

B. A. Scott, G. R. Eulenberger, and R. A. Bernheim, J. Chem. Phys. **48**, 263 (1968)

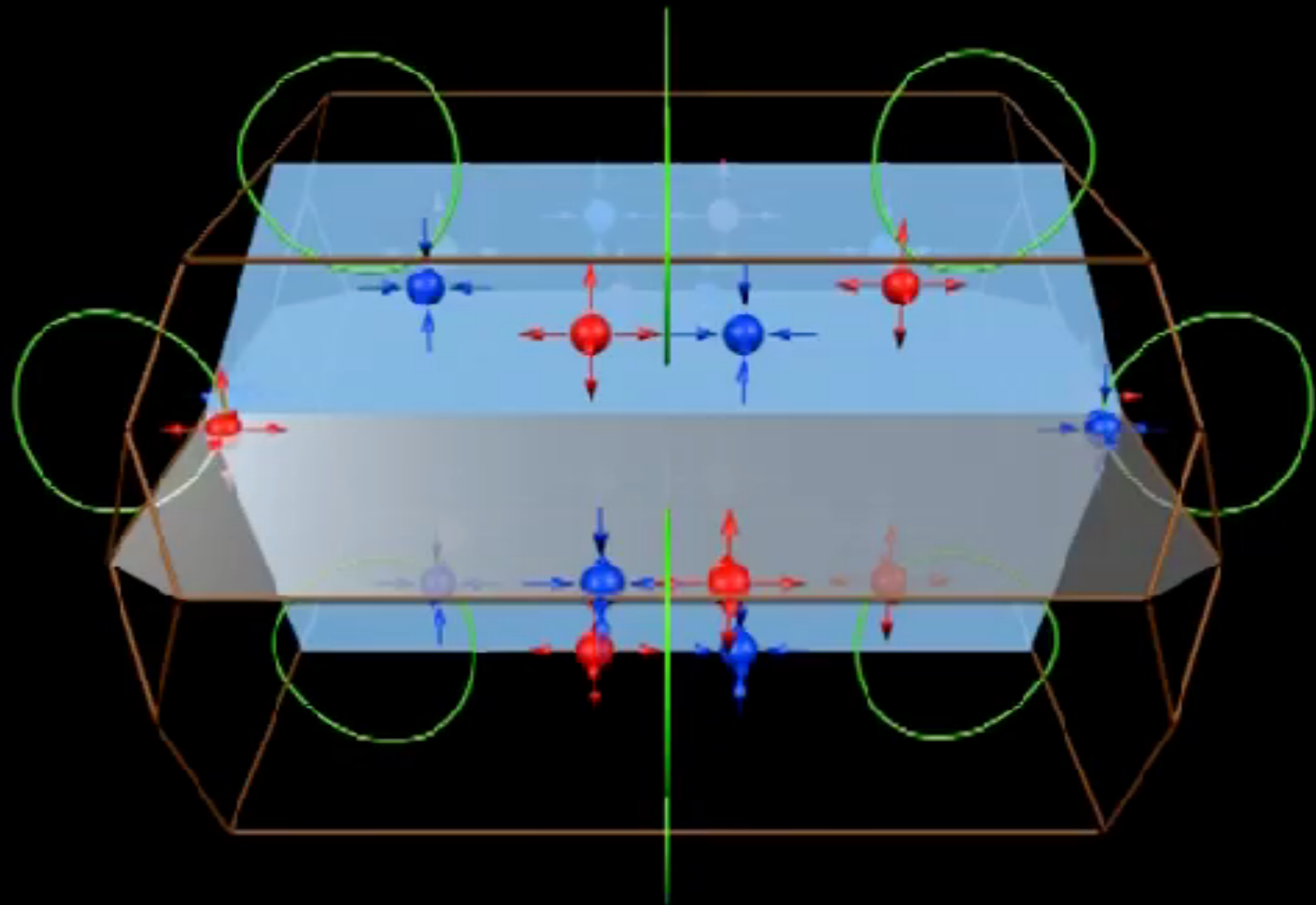
Band structure of TaAs



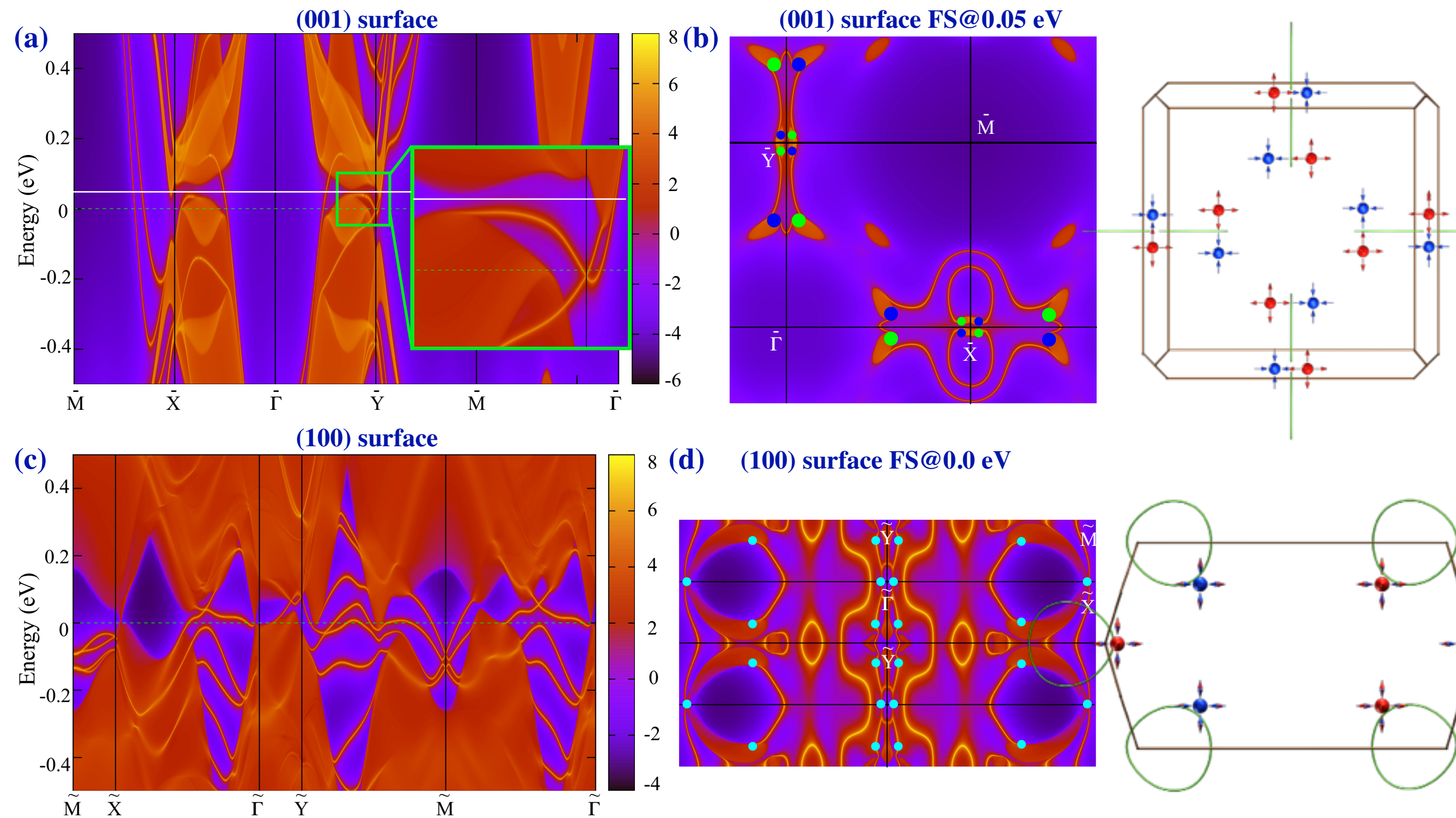
Topological Node-Line
Semimetal

<http://arxiv.org/abs/1411.2175>

3D View



Surface Fermi arcs



Experimental verification

up to early of Apr. 2015 from arXiv.

- 1 [2015arXiv:1502.00251](https://arxiv.org/abs/1502.00251) Tantalum Monoarsenide: an Exotic Compensated Semimetal
- 2 [2015arXiv:1502.03807](https://arxiv.org/abs/1502.03807) Experimental realization of a topological Weyl semimetal phase with Fermi arc surface states in TaAs
@Science on Jul. 16, 2015 from Princeton & Peking University
- 3 [2015arXiv:1502.04361](https://arxiv.org/abs/1502.04361) Extremely large magnetoresistance and ultrahigh mobility in the topological Weyl semimetal NbP
- 4 [2015arXiv:1502.04684](https://arxiv.org/abs/1502.04684) **Discovery of Weyl semimetal TaAs**
@PRX on Jul. 16 from IOP, CAS
- 5 [2015arXiv:1503.01304](https://arxiv.org/abs/1503.01304) **Observation of the chiral anomaly induced negative magneto-resistance in 3D Weyl semi-metal TaAs**
@PRX on Jul. 20 from IOP, CAS
- 6 [2015arXiv:1503.02630](https://arxiv.org/abs/1503.02630) Observation of the Adler-Bell-Jackiw chiral anomaly in a Weyl semimetal
- 7 [2015arXiv:1503.07571](https://arxiv.org/abs/1503.07571) Magnetotransport of single crystalline NbAs
- 8 [2015arXiv:1503.09188](https://arxiv.org/abs/1503.09188) **Observation of Weyl nodes in TaAs**
@Nat. Phys. on Aug. 17 from IOP, CAS
- 9 [2015arXiv1504.01350](https://arxiv.org/abs/1504.01350) Discovery of Weyl semimetal NbAs
@Nat. Phys. on Aug. 17 from Princeton & Peking University

Four hallmarks of Weyl semimetal observed in TaAs

1. “Chiral anomaly”— negative magnetoresistance

[arXiv:1503.01304](#) **Observation of the chiral anomaly induced negative magneto-resistance in 3D Weyl semi-metal TaAs** IOP, CAS group

[arXiv:1503.02630](#) Observation of the Adler-Bell-Jackiw chiral anomaly in a Weyl semimetal PU&PKU group

2. Fermi arcs

[arXiv:1502.03807](#) Experimental realization of a topological Weyl semimetal phase with Fermi arc surface states in TaAs PU&PKU group

[arXiv:1502.04684](#) **Discovery of Weyl semimetal TaAs** IOP, CAS group

3. Bulk Weyl nodes

[arXiv:1502.03807](#) Experimental realization of a topological Weyl semimetal phase with Fermi arc surface states in TaAs

[arXiv:1503.09188](#) **Observation of Weyl nodes in TaAs** IOP, CAS group PU&PKU group

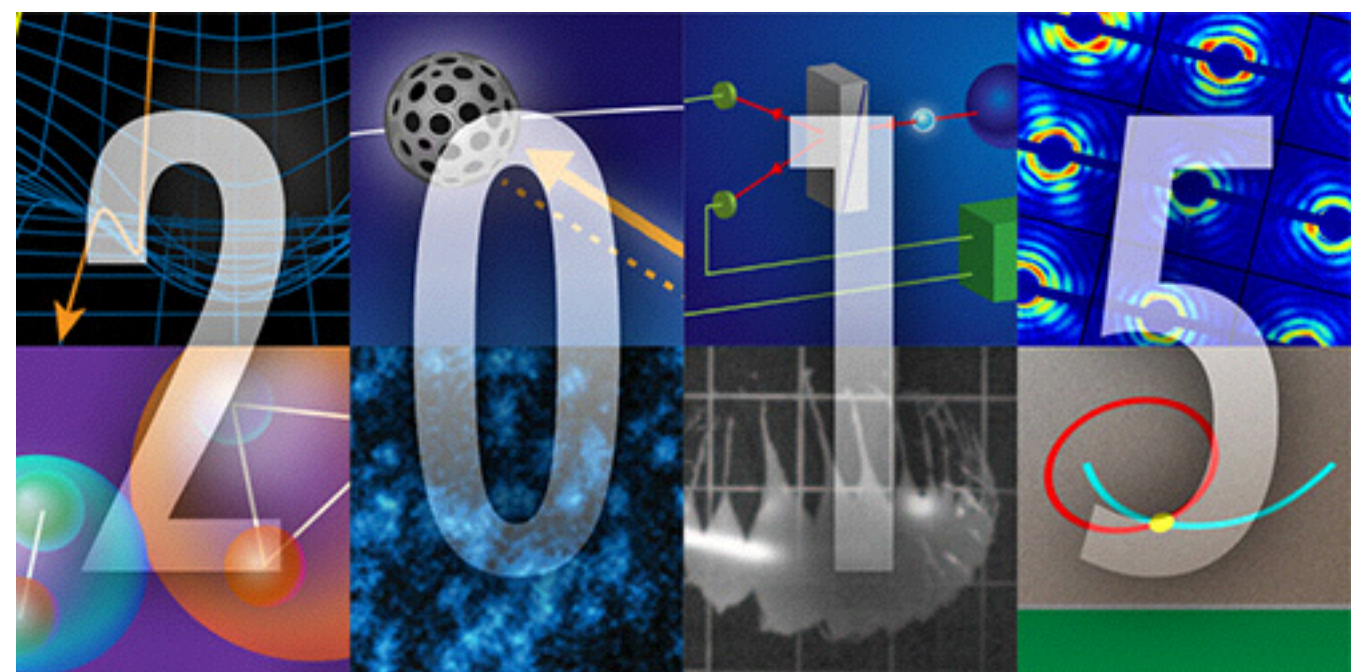
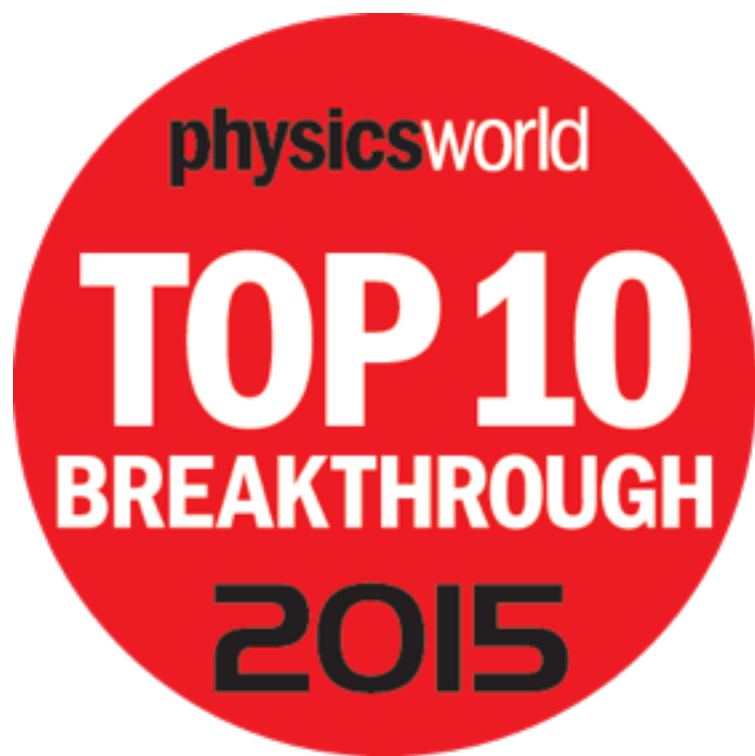
4. Spin texture of Fermi arc

[arXiv:1510.07256](#) **Observation of spin texture of Fermi arc of TaAs** IOP, CAS group

Breakthrough & Highlight of 2015

Weyl fermions are spotted at long last

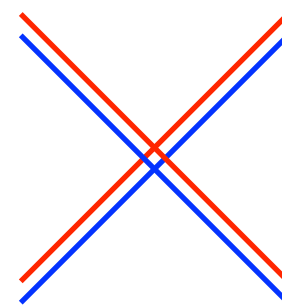
To Zahid Hasan of Princeton University, Marin Soljačić of MIT, and Zhong Fang and Hongming Weng of the Chinese Academy of Sciences, for their pioneering work on Weyl fermions. These massless particles were predicted by the German mathematician Hermann Weyl in 1929. Working independently, a team led by Hasan, and another led by Fang and Weng, spotted telltale evidence



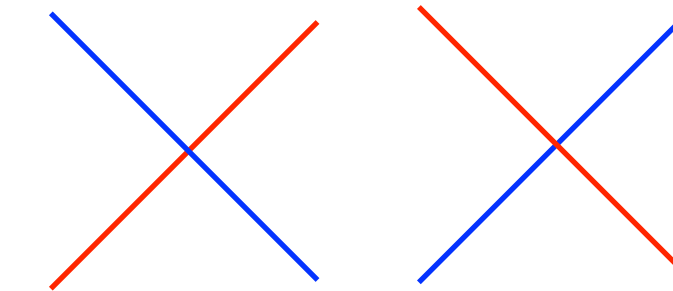
Triply Degenerate Nodal Point

A New Massless Fermion

Weng, Fang, et al., PRB **93**, 241202(R) (2016)



DSM
(4x4)

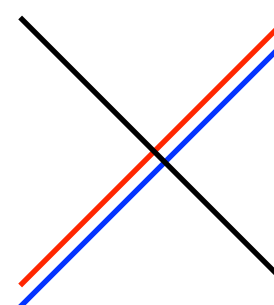


WSM
(2x2)

		E	C2	2C3	2C6	3IC2`	3IC2"
G1	A1	1	1	1	1	1	1
G2	A2	1	1	1	1	-1	-1
G3	B1	1	-1	1	-1	1	-1
G4	B2	1	-1	1	-1	-1	1
G5	E1	2	-2	-1	1	0	0
G6	E2	2	2	-1	-1	0	0

		E1/2	0	1	/3	0	0
G7	E1/2	2	0	1	/3	0	0
G8	E5/2	2	0	1	-/3	0	0
G9	E3/2	2	0	-2	0	0	0

Na₃Bi Γ -A C_{6v}

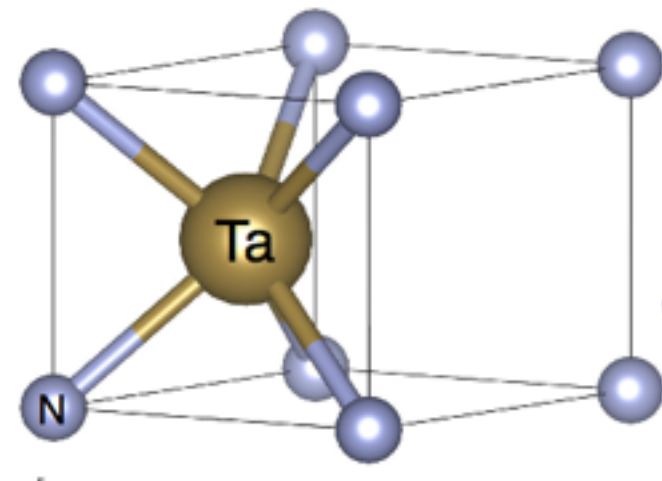


TDNP
(3x3)

Point group C _{3v}		E	2C3	3IC2
G1	A1	1	1	1
G2	A2	1	1	-1
G3	E	2	-1	0

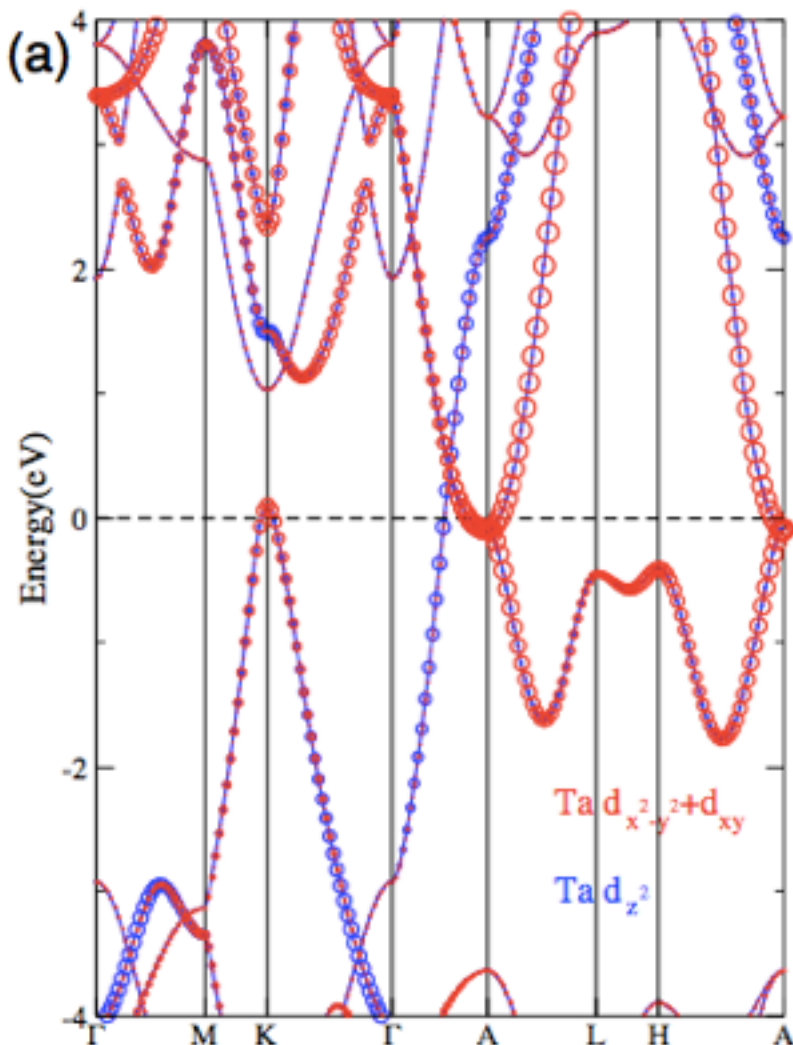
G4	E1/2	2	1	0
G5	1E3/2	1	-1	i
G6	2E3/2	1	-1	-i

Triply Degenerate Nodal Point

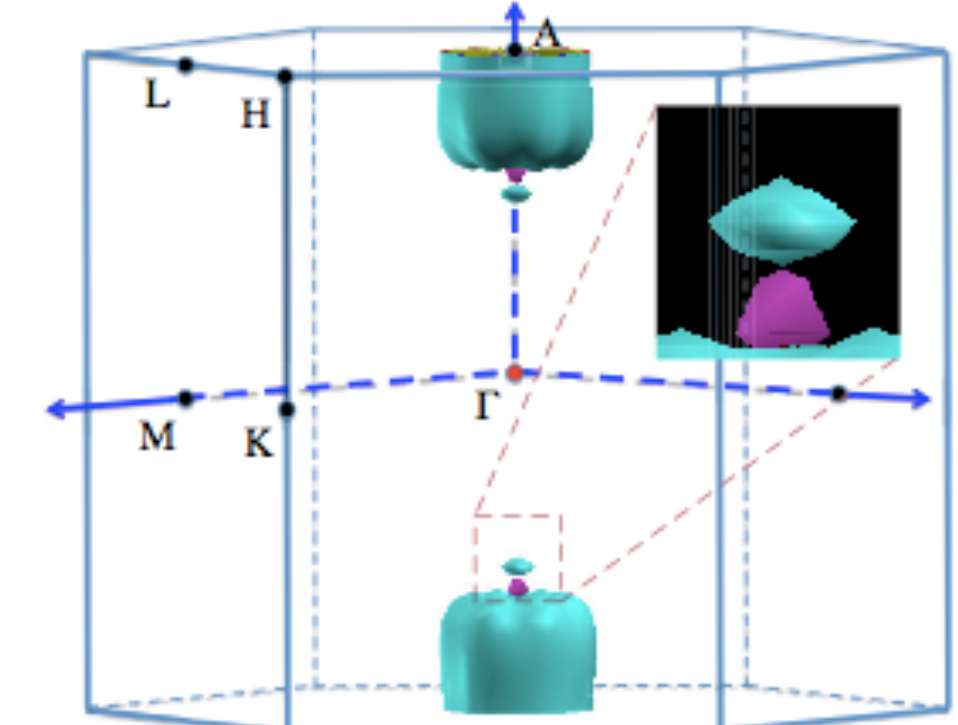
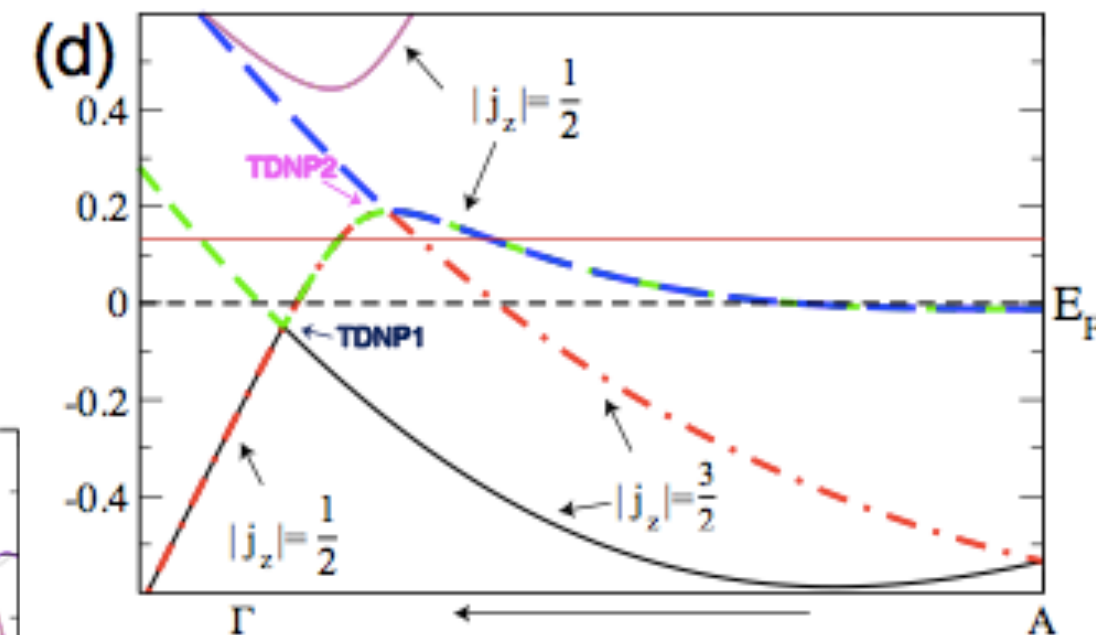
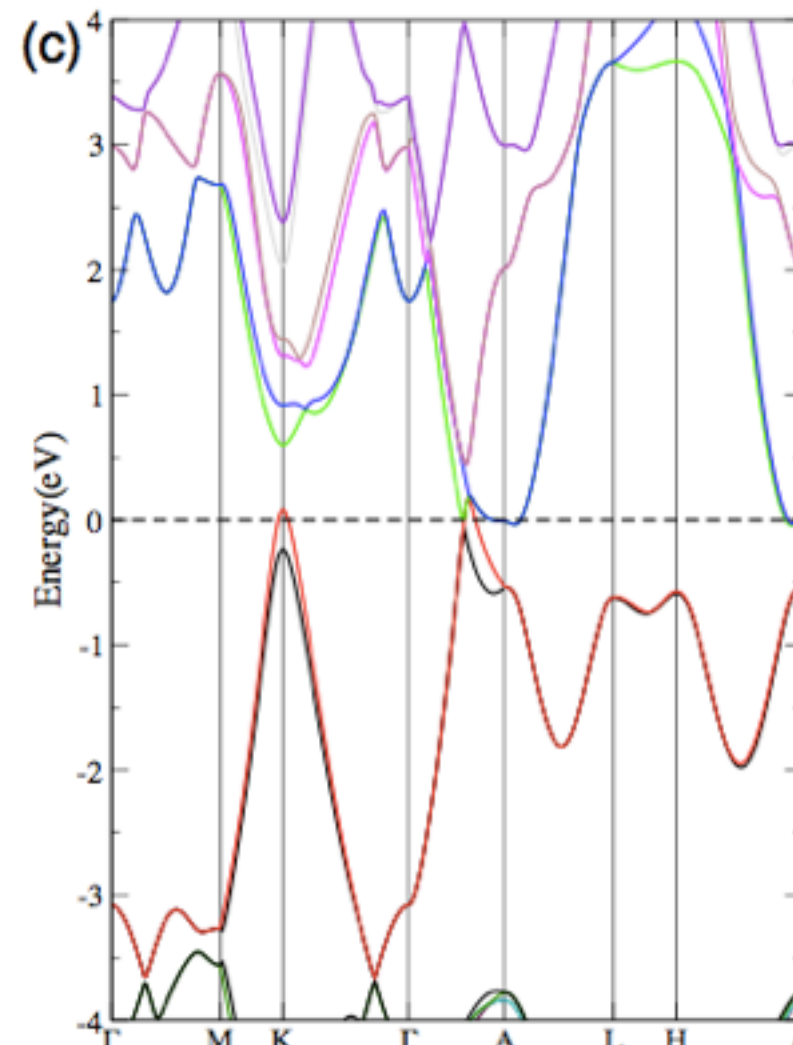


WC-type
TaN, NbN, ZrTe etc.

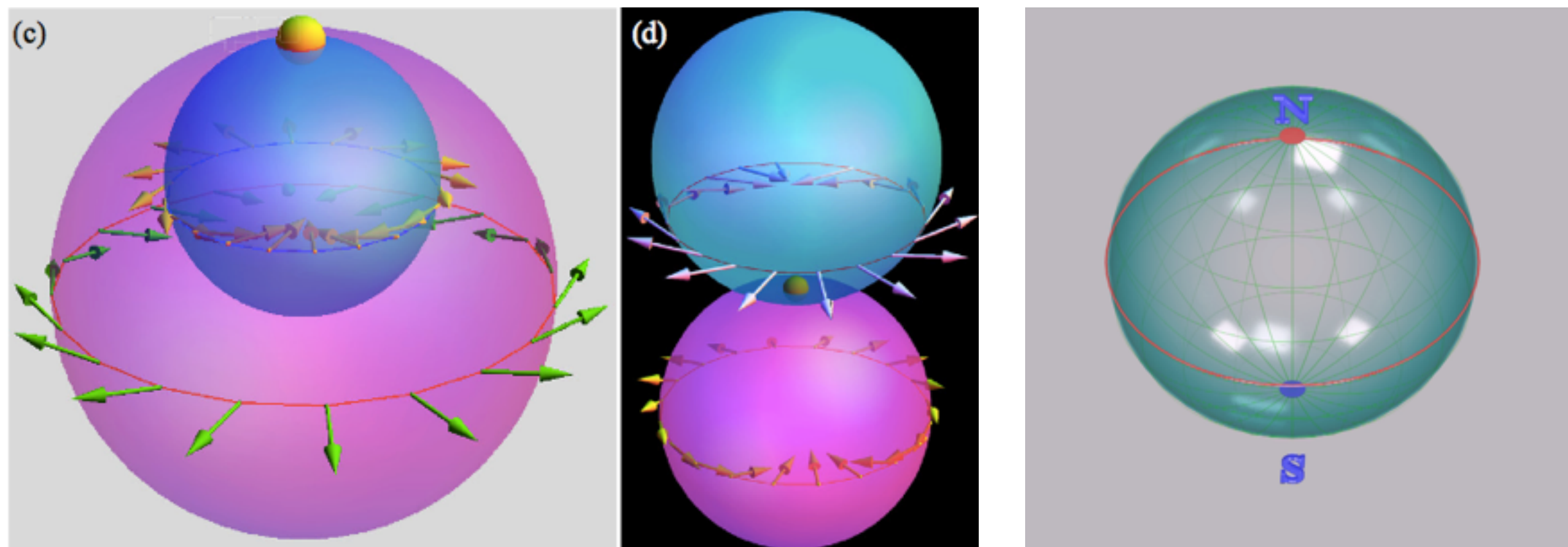
No SOC



+SOC



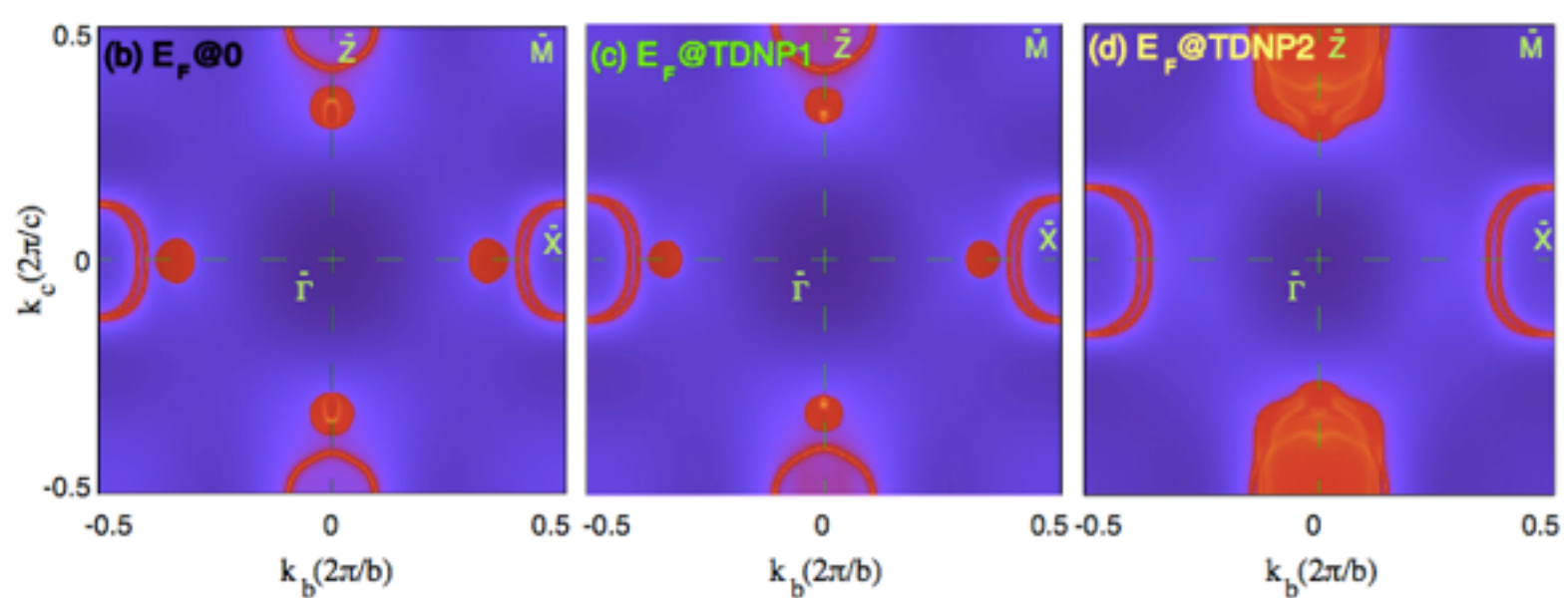
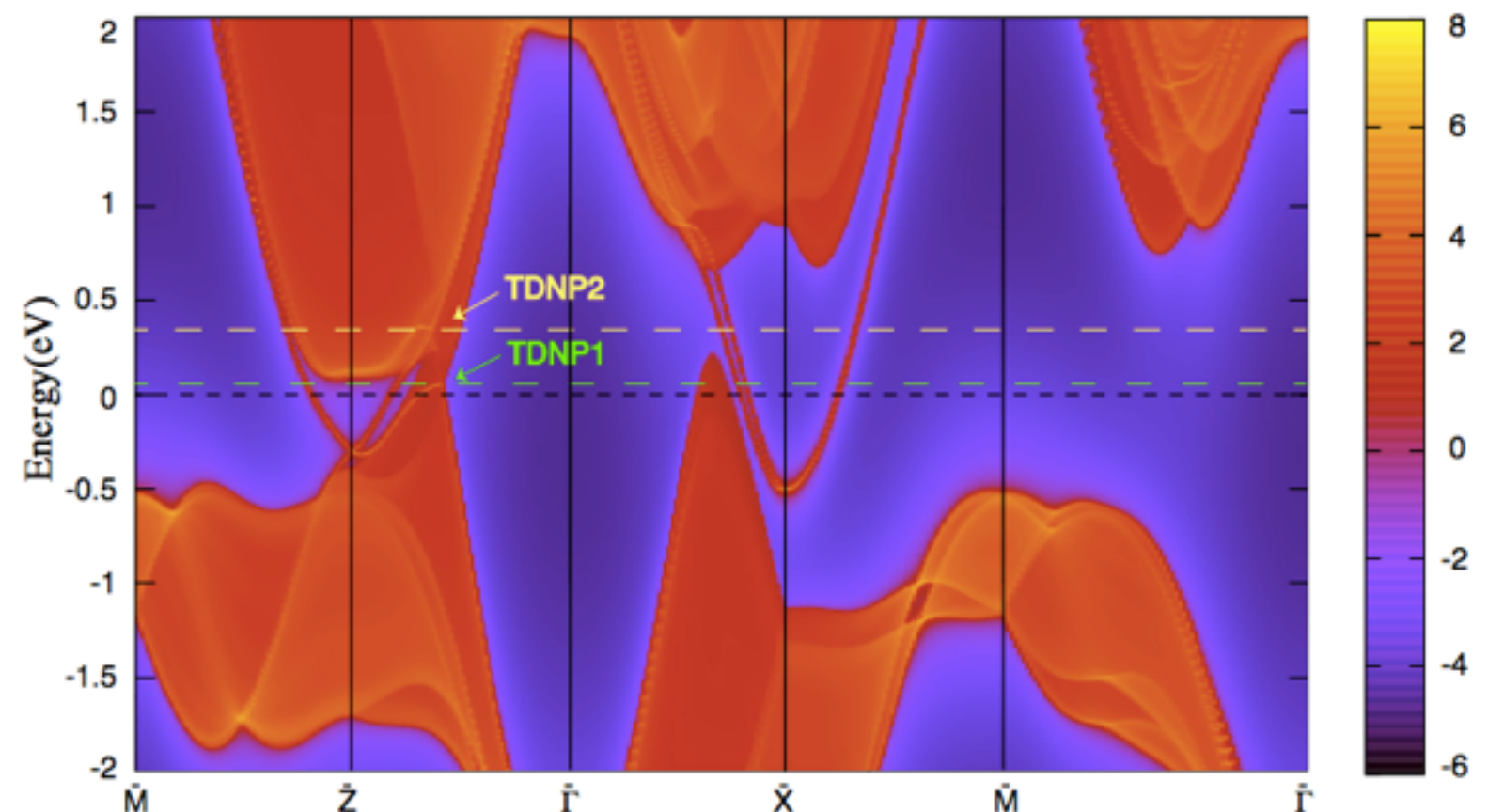
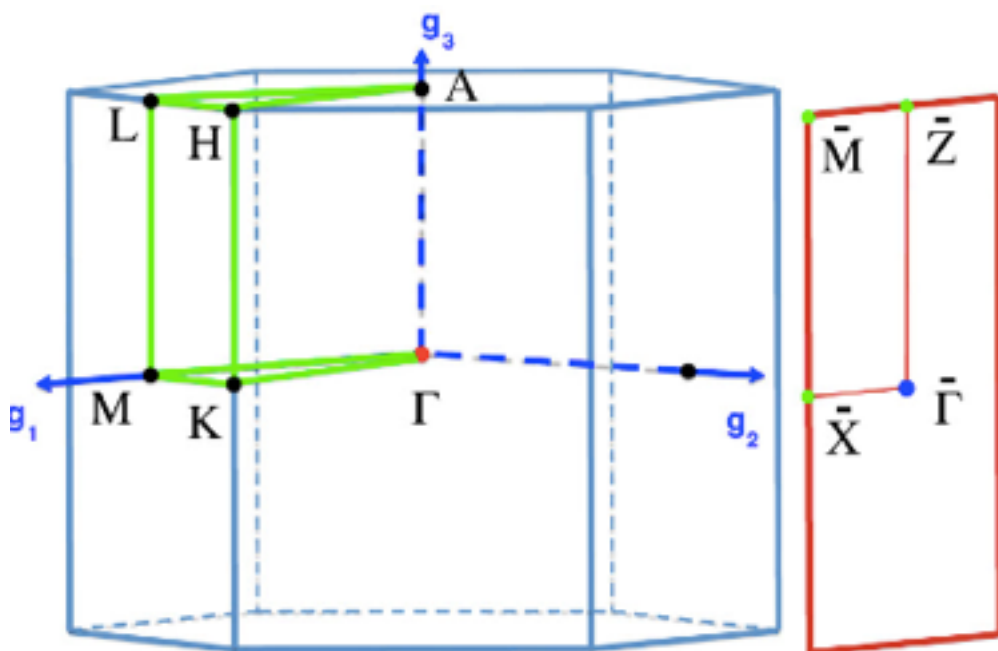
Triply Degenerate Nodal Point



Winding number 2 for spin on the Fermi surface

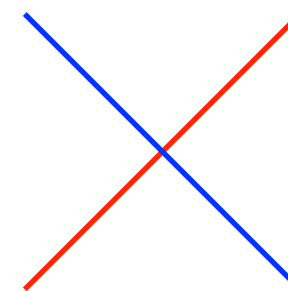
Triply Degenerate Nodal Point

(100) surface

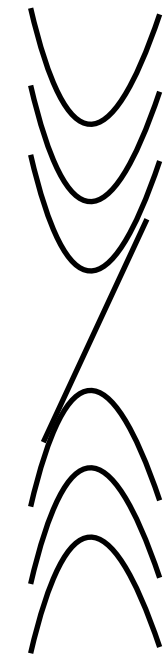
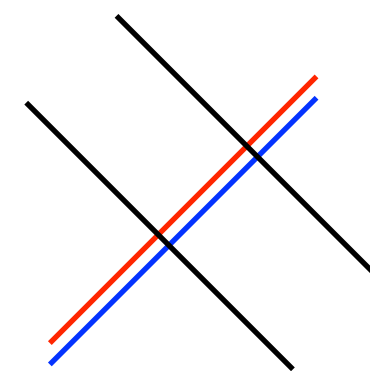


Triply Degenerate Nodal Point

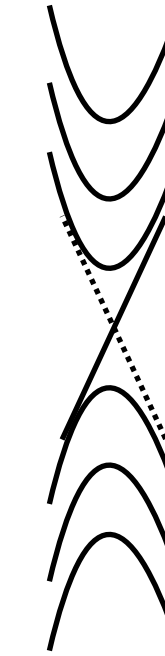
B



B/c



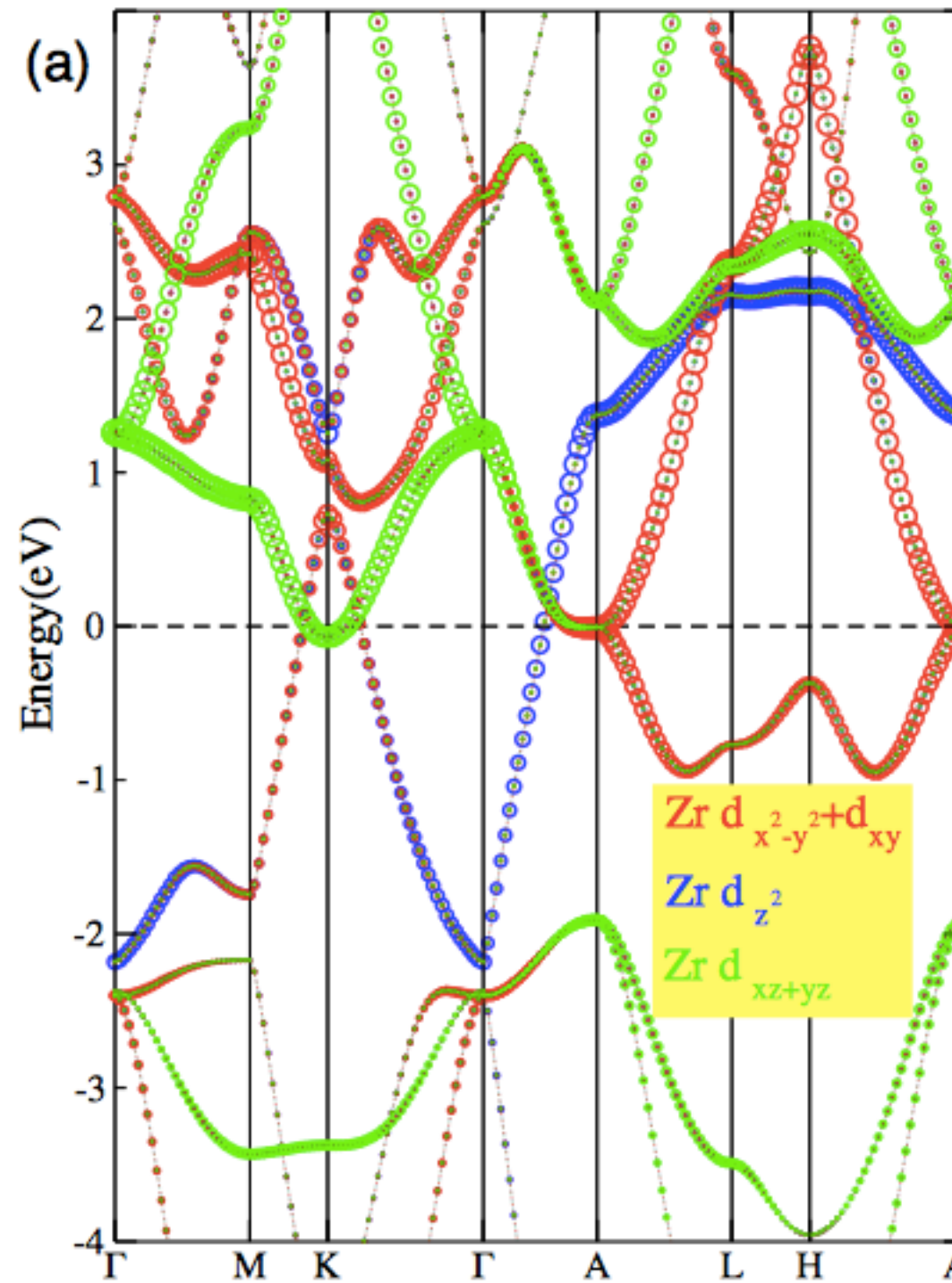
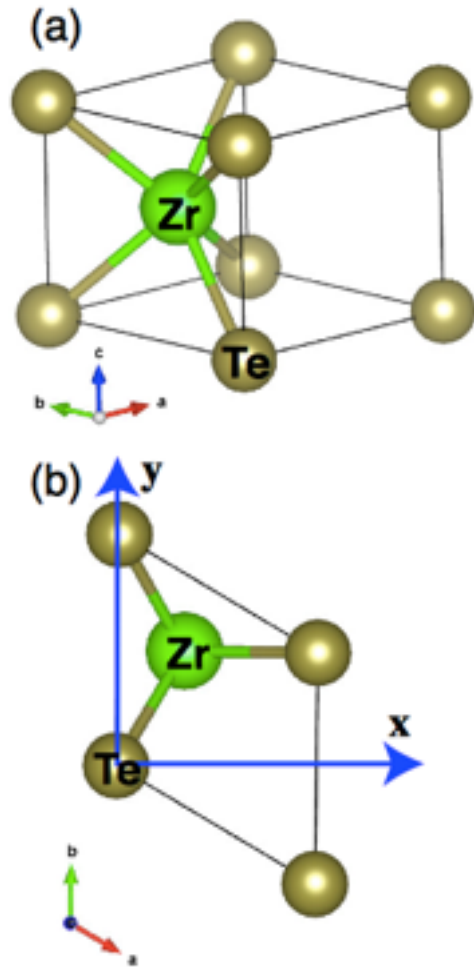
Chiral anomaly



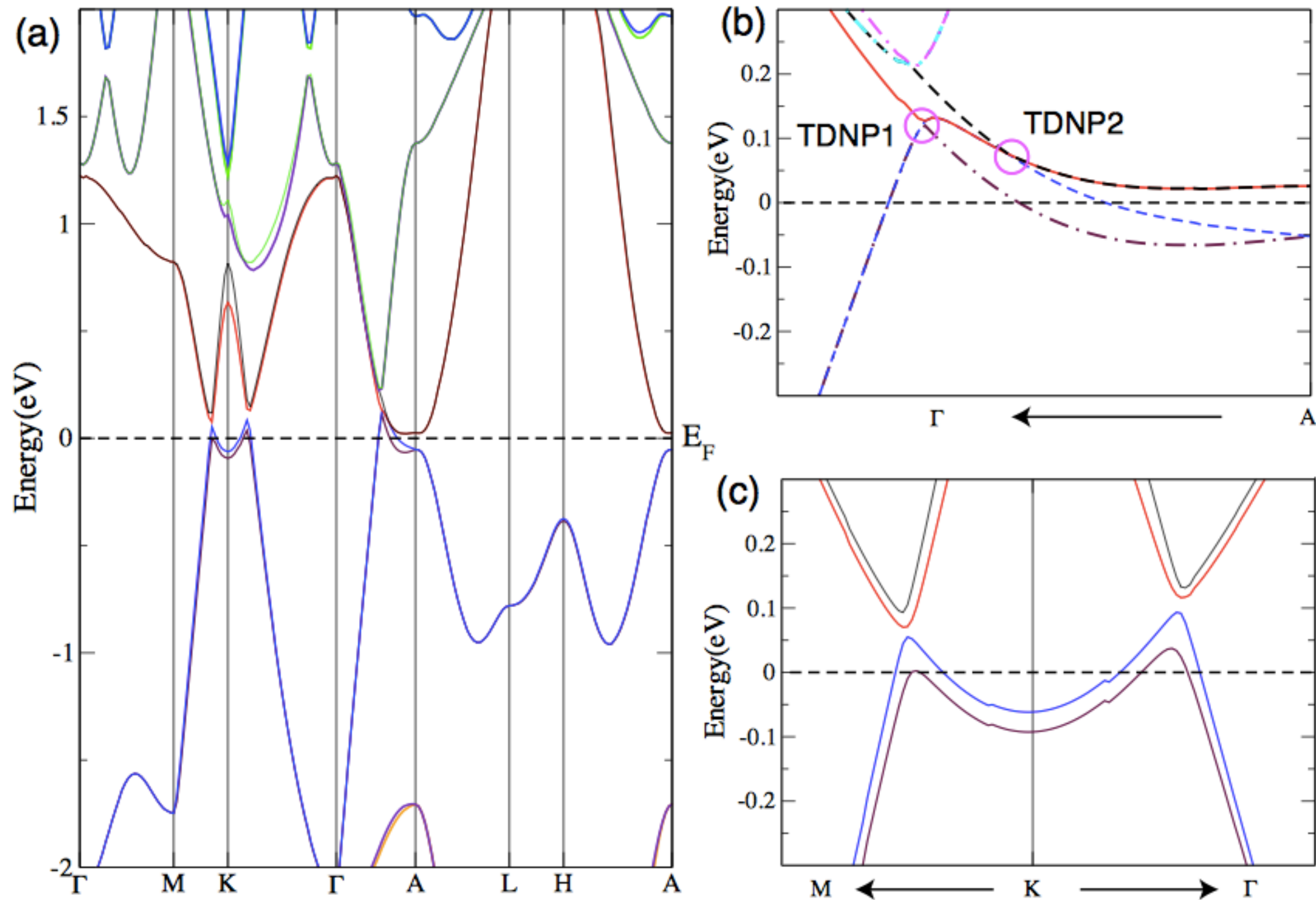
Helical anomaly

Protected by C_3

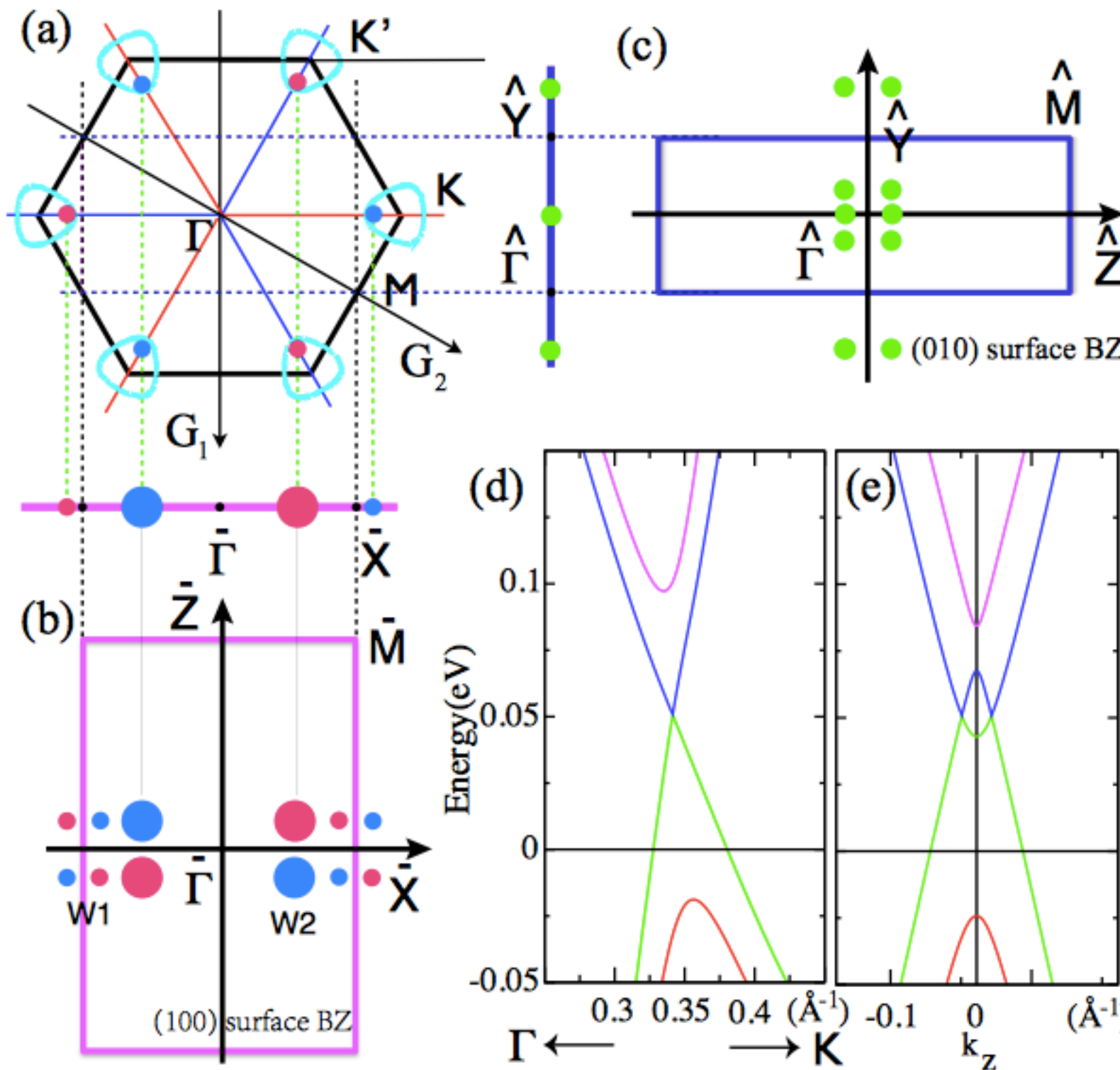
Weyl nodal points Co-exist with Triply Degenerate Nodal Points



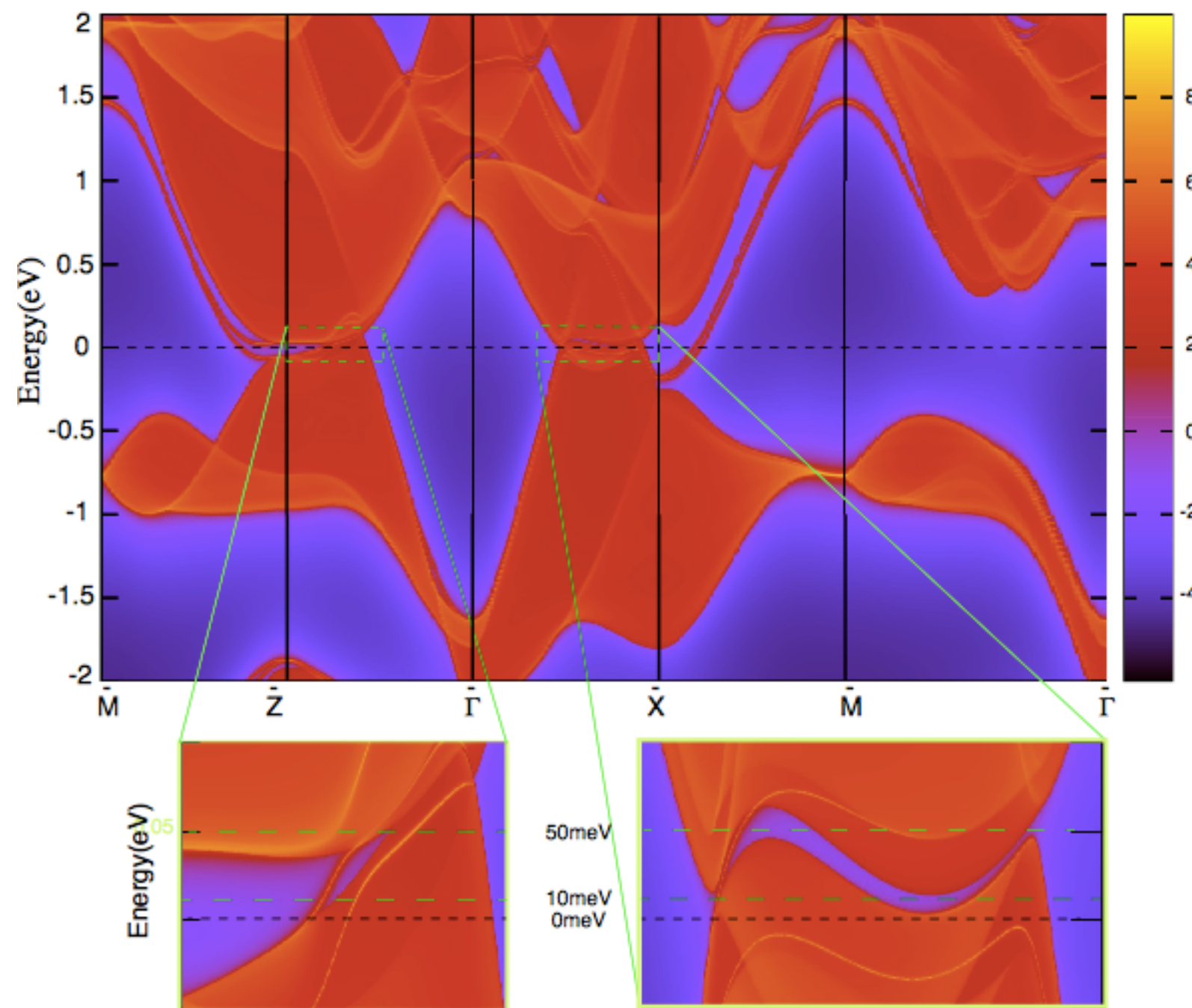
Weyl points co-exist with Triply Degenerate Nodal Points



Weyl points co-exist with Triply Degenerate Nodal Points

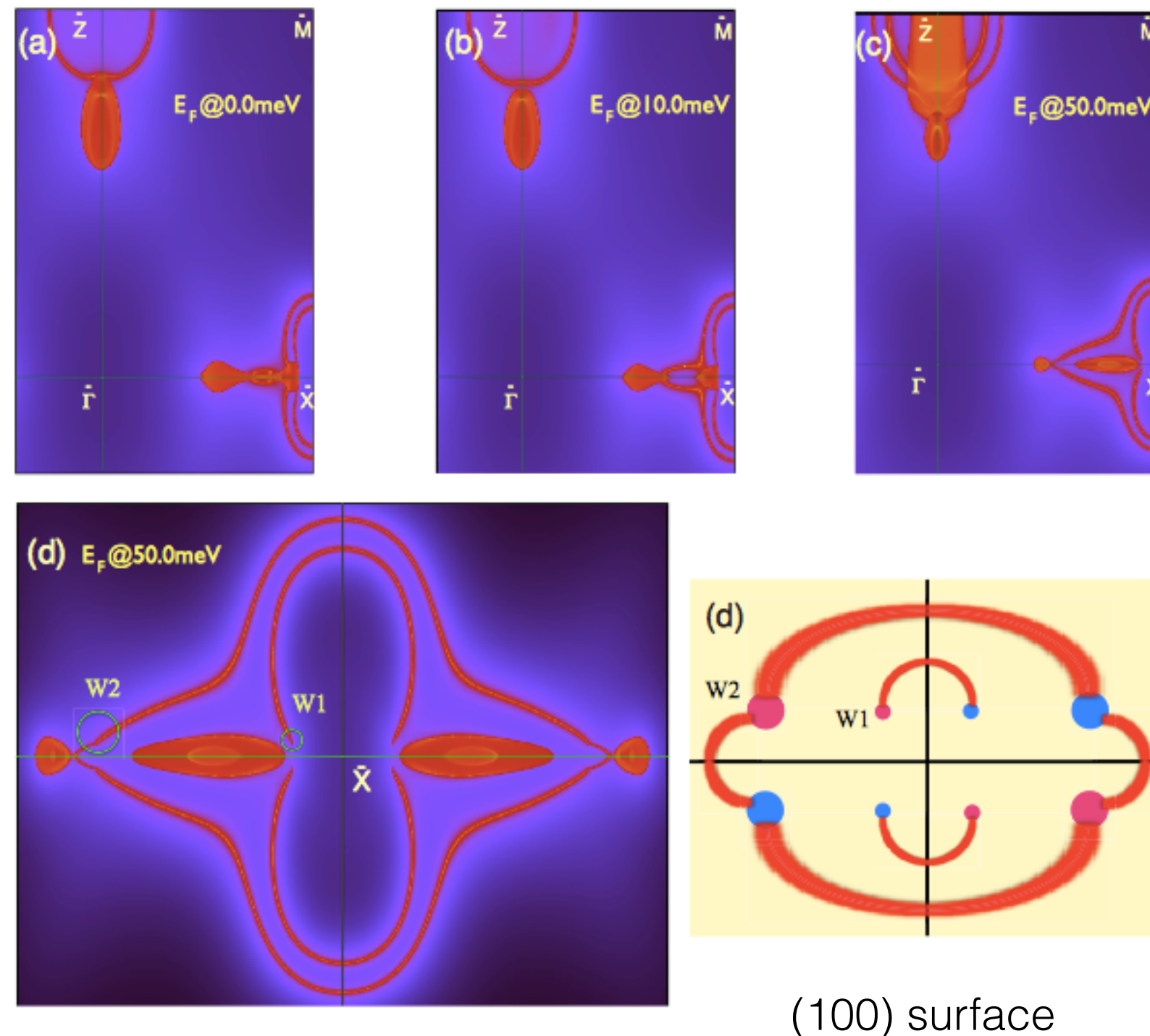


Weyl points co-exist with Triply Degenerate Nodal Points

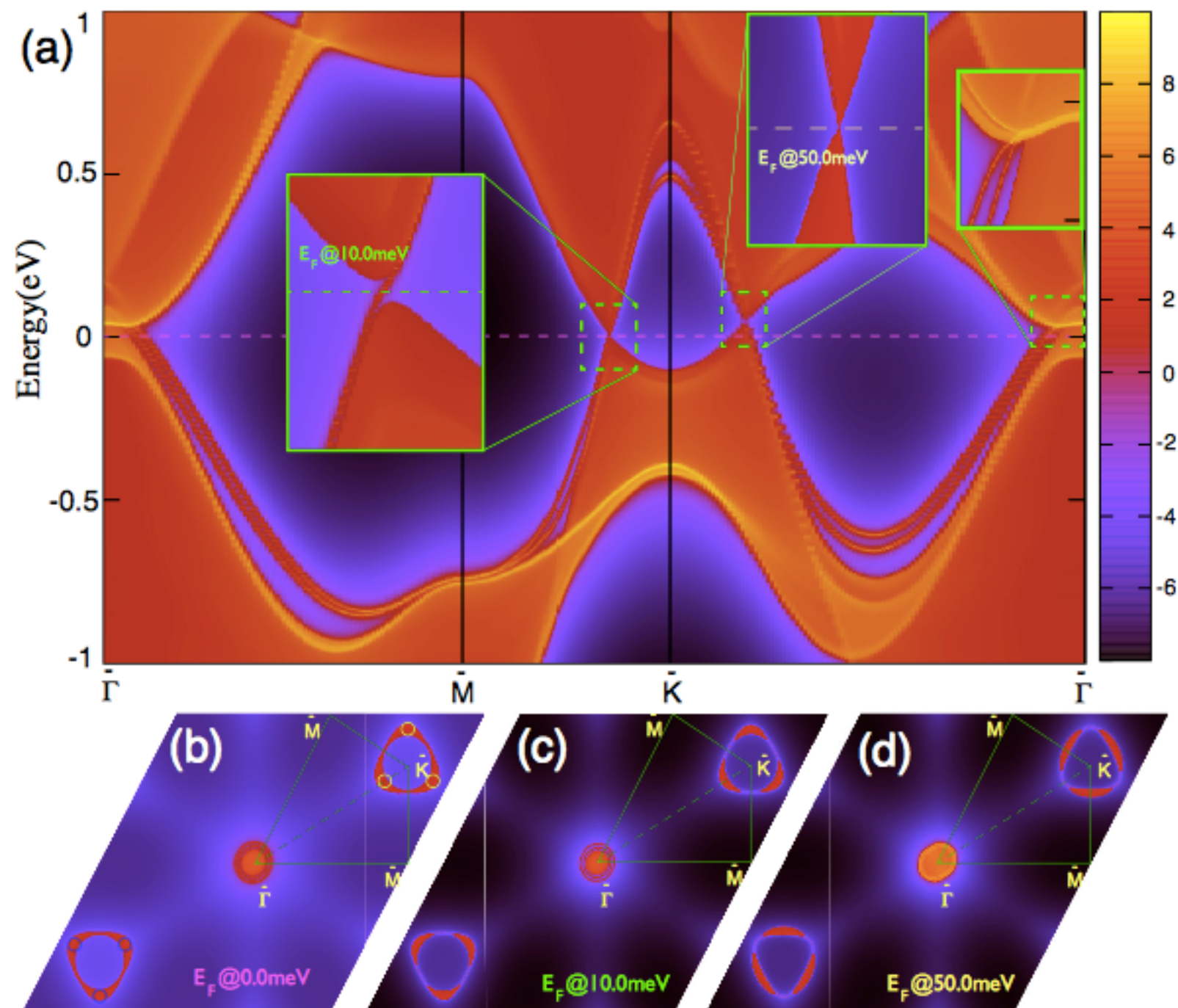


(Color online) ZrTe (100) surface state with its band structure weighted

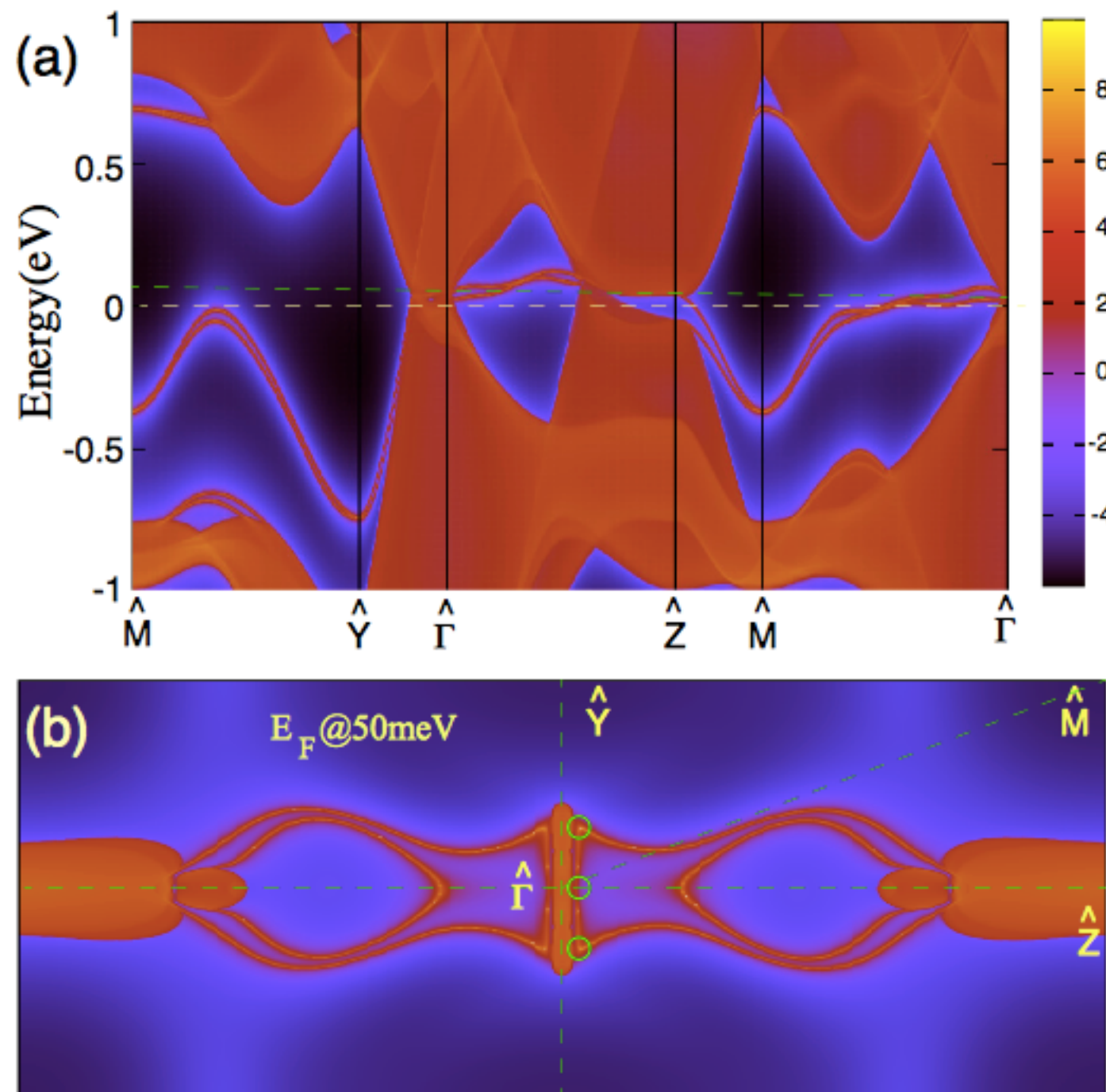
Weyl points co-exist with Triply Degenerate Nodal Points



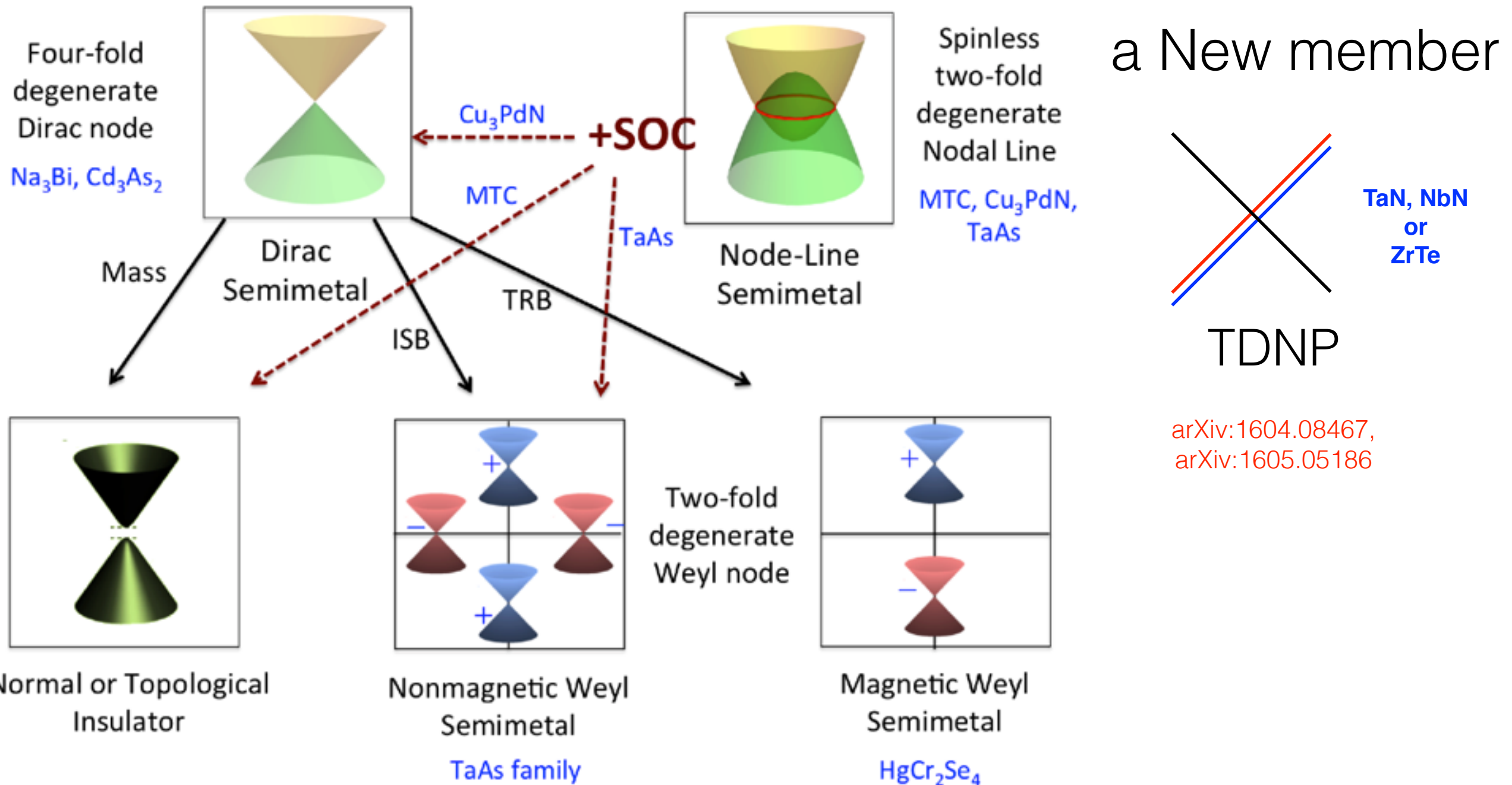
Weyl points co-exist with Triply Degenerate Nodal Points



Weyl points co-exist with Triply Degenerate Nodal Points



Topological Semimetal Family



Topological Quantum State

???

single particle

Topological insulator

Topo.
crys. insul.

Chern insulator
(QAHE)

I-QHE

Topological
Semimetal

Weyl

Dirac

Node
Line

Metal

Many-body
correlation

Topol.
Kondo
Insulator

Topol. Crys.
Kondo Insul.

Topol.
Supercond.

F-TI

F-QHE

Thank you for your attention !